

***Nurhachius luei*, a new istiodactylid pterosaur (Pterosauria, Pterodactyloidea) from the Early Cretaceous Jiufotang Formation of Chaoyang City, Liaoning Province (China) and comments on the Istiodactylidae**

Xuanyu Zhou^{Corresp., 1, 2}, Rodrigo V. Pêgas^{Corresp., 3}, Maria E. C. Leal^{4, 5}, Niels Bonde^{5, 6}

¹ Institute of Geology, Chinese Academy of Geological Sciences, Beijing, China

² China University of Geosciences, Beijing, China

³ Laboratory of Vertebrate Paleontology and Animal Behavior, Universidade Federal do ABC, São Bernardo, São Paulo, Brazil

⁴ Departamento de Geologia, Universidade Federal do Ceará, Fortaleza, Ceará, Brazil

⁵ Zoological Museum (SNM), Copenhagen University, Copenhagen, Denmark

⁶ Fur Museum (Museum Saling), Fur, Denmark

Corresponding Authors: Xuanyu Zhou, Rodrigo V. Pêgas

Email address: zhouxu2017@yeah.net, rodrigo.pegas@hotmail.com

A new istiodactylid pterosaur, *Nurhachius luei* sp. nov., is here reported based on a complete skull with mandible and some cervical vertebrae from the lower part of the Jiufotang Formation of western Liaoning (China). This is the second species of *Nurhachius*, the type-species being *N. ignaciobrito* from the upper part of the Jiufotang Formation. A revised diagnosis of the genus *Nurhachius* is provided, being this taxon characterized by the presence of a slight dorsal deflection of the palatal anterior tip, which is homoplastic with the *Anhangueria* and *Cimoliopterus*. *Nurhachius luei* sp. nov. shows an unusual pattern of tooth replacement, with respect to other pterodactyloid species. The relationships within the Istiodactylidae and with their closest taxa are investigated through a phylogenetic analysis by parsimony.

1 ***Nurhachius luei*, a new istiodactylid pterosaur**
2 **(Pterosauria, Pterodactyloidea) from the Early**
3 **Cretaceous Jiufotang Formation of Chaoyang City,**
4 **Liaoning Province (China); and comments on the**
5 **Istiodactylidae**

6 Xuanyu Zhou^{1,2}, Rodrigo Vargas Pêgas³, Maria Eduarda de Castro Leal^{4,5}, Niels Bonde^{5,6}

7

8 1. Institute of Geology, Chinese Academy of Geological Sciences, Beijing, China

9 2. China University of Geosciences, Beijing, China

10 3. Laboratory of Vertebrate Paleontology and Animal Behavior, Universidade Federal do ABC,
11 São Bernardo, São Paulo, Brazil

12 4. Departamento de Geologia, Universidade Federal do Ceará, Fortaleza, Ceará, Brazil

13 5. Zoological Museum (SNM), Copenhagen University, Copenhagen, Denmark

14 6. Fur Museum (Museum Saling), Fur, Denmark

15

16 Corresponding Author:

17 Xuanyu Zhou

18 No.26 Baiwanzhuang Street, Beijing, Beijing, 100037, China

19 Email address: zhouxy2017@yeah.net

20 Rodrigo Vargas Pêgas

21 Alameda da Universidade, s/n - Anchieta, São Bernardo do Campo - SP, 09606-045, Brazil

22 Email address: rodrigo.pegas@hotmail.com

23

24 **Abstract**

25 A new istiodactylid pterosaur, *Nurhachius luei* sp. nov., is here reported based on a complete skull
26 with mandible and some cervical vertebrae from the lower part of the Jiufotang Formation of
27 western Liaoning (China). This is the second species of *Nurhachius*, the type-species being *N.*
28 *ignaciobrito* from the upper part of the Jiufotang Formation. A revised diagnosis of the genus
29 *Nurhachius* is provided, being this taxon characterized by the presence of a slight dorsal deflection
30 of the palatal anterior tip, which is homoplastic with the *Anhangueria* and *Cimoliopterus*.

31 *Nurhachius luei* sp. nov. shows an unusual pattern of tooth replacement, with respect to other
32 pterodactyloid species. The relationships within the Istiodactylidae and with their closest taxa are
33 investigated through a phylogenetic analysis by parsimony.

34 **Introduction**

35 Istiodactylid pterosaurs are characterized by rhombic teeth with lancet-shaped crowns, long skulls
36 with short pre-antorbital portions of the rostrum, and nasoantorbital fenestrae representing over 50
37 percent of the total skull length and height (Howse *et al.*, 2001; Andres & Ji, 2006; Lü *et al.*, 2013).
38 The group was originally named by Howse *et al.* (2001) in order to accommodate, then, only
39 *Istiodactylus latidens*. Later, the Istiodactylidae were phylogenetically defined by Andres *et al.*
40 (2014) as the least inclusive clade containing *Nurhachius* and *Istiodactylus*.

41 Four pterosaur genera and five species (all represented by a single specimen) have been referred
42 to the Istiodactylidae sensu Andres *et al.* (2014) in the literature, namely *Istiodactylus latidens*, *I.*
43 *sinensis*, *Liaoxipterus brachyognathus*, *Nurhachius ignaciobritoi* and *Longchengpterus zhaoi*.
44 However, *Longchengpterus zhaoi* has been considered a junior synonym of *N. ignaciobritoi* by Lü
45 *et al.* (2008), a view that is followed here (see Discussion). Therefore, *N. ignaciobritoi* is the only
46 Chinese istiodactylid species to be represented by two specimens so far. *Haopterus gracilis*,
47 *Hongshanopterus lacustris* and *Archaeoistiodactylus linglongtaensis* have been reported in
48 literature as taxa that are close to the Istiodactylidae (Wang XL & Lü, 2001; Wang XL *et al.*,
49 2008a; Lü & Fucha, 2010). However, the affinity of *Archaeoistiodactylus linglongtaensis* has been
50 questioned by Sullivan *et al.* (2014).

51 All istiodactylid pterosaurs are from the Early Cretaceous Jiufotang Formation of northeastern
52 China with the exception of *Istiodactylus latidens*, which is from the Early Cretaceous Vectis
53 Formation of the Isle of Wight, Southern England. Also, the three taxa that are reported as close
54 to istiodactylids come from northeastern China and surrounding areas: *Haopterus gracilis* is
55 from the Early Cretaceous Yixian Formation, *Hongshanopterus lacustris* from the Jiufotang
56 Formation, and *Archaeoistiodactylus linglongtaensis* from the Middle Jurassic Tiaojishan
57 Formation. Apart from the latter, these Chinese pterosaurs belong to the Jehol Biota (see Chang
58 *et al.*, 2003).

59 By the end of 2016, 23 species of pterosaurs from the Jiufotang Formation have been reported

60 (Andres & Ji, 2006; Dong & Lü, 2005; Dong *et al.*, 2003; Jiang *et al.*, 2016; Rodrigues *et al.*,
61 2015; Li *et al.*, 2003; Lü & Ji, 2005; Lü & Yuan, 2005; Lü *et al.*, 2006, 2007, 2008, 2016a,
62 2016b; Wang L *et al.*, 2006; Wang XL & Zhou, 2003a, 2003b; Wang XL *et al.*, 2005, 2008a,
63 2008b, 2012, 2014).

64 In this paper, we describe a second species of *Nurhachius* from the Jiufotang Formation and
65 investigate the phylogenetic relationships of the istiodactylids and purported close taxa.

66

67 **Geological, paleontological and geochronological information**

68 The Jiufotang Formation is known worldwide for its paleontological richness and the exquisite
69 preservation of its fossils, which include plants, insects, fishes, mammals, birds, non-avian
70 dinosaurs and pterosaurs (Wang X, 2018; Meng *et al.*, 2011; Wang M and Zhou, 2019; Yao *et al.*,
71 2019). Fossils occur mainly in the lower part of the formation, known as Boluochi Beds or
72 Boluochi Member (see Chang *et al.*, 2003), which is characterized by the *Jinanichthys* –
73 *Cathayornis* Fauna that includes small feathered dinosaurs like the four-winged *Microraptor* (Xu
74 *et al.*, 2003) and several pterosaurs (Chang *et al.*, 2003; Zhou *et al.*, 2003).

75 The Jiufotang Formation is 206–2685 m thick according to Chang *et al.* (2009) and is mainly
76 composed of mudstone, siltstone, shale, sandstone and tuff. A tuff from the basal part of formation
77 (two meters above the boundary between the Yixian and Jiufotang formations) in western Liaoning
78 was dated to 122.1 ± 0.3 Ma by Chang *et al.* (2009). A basalt in the upper part of the formation in
79 Inner Mongolia was dated to 110.59 ± 0.52 Ma by Eberth *et al.* (1993), but Chang *et al.* (2009)
80 objected that the correlation between the Jiufotang Formation in Liaoning and Inner Mongolia is
81 unclear and the age of the uppermost Jiufotang Formation remains unknown. The Aptian age of
82 the Early Cretaceous ranges ~125–113 Ma according to the International Chronostratigraphic Chart
83 2018/08. Therefore, the Jiufotang Formation is Aptian in age, but might reach the Albian.

84 The Jiufotang Formation and the underlying Yixian Formation traditionally constitute the Jehol
85 Group. The Yixian Formation is 225–4000 m thick, varying in thickness and lithology in different
86 areas according to Chang *et al.* (2009), but only a fraction is made of sedimentary rocks because
87 basalts and lavas represents a substantial part of the section. Chang *et al.* (2009) dated the basal
88 part of the Yixian Formation in Western Liaoning to 129.7 ± 0.5 and the uppermost part of the

89 underlying Tuchengzi Formation to 139.5 ± 1.0 Ma. The upper part of the Yixian Formation (the
90 Jingangshan Beds) was dated to 126.5 Ma (Chang *et al.*, 2003). Therefore, the Yixian Formation
91 represents an interval of ~ 7 Ma from early Barremian to early Aptian and the Jiufotang Formation
92 might represents an interval of over 11 Ma from early Aptian to early Albian.

93 The Jehol Group has yielded the famous Jehol biota. Four fossil-bearing levels with partly different
94 fossil associations have been distinct within the Yixian Formation and only one (corresponding to
95 the Boluochi Beds) in the Jiufotang Formation (Chang *et al.* 2003).

96 Both the holotype of *N. ignaciobritoi* and its referred specimen (the holotype of *Longchengpterus*
97 *zhaoi*) come from the upper part of the Jiufotang Formation (see Wu *et al.*, 2018), whereas the new
98 species comes from the Boluochi Beds (lower part of the Jiufotang Formation).

99

100 **Material & Methods**

101 The holotype and only specimen of the new species consists of a skull with mandible and seven
102 articulated cervical vertebrae. It was previously figured in Lü *et al.* (2013, figures at pp. 81-82)
103 and reported as an unnamed istiodactylid. The specimen was found near the village of
104 Huanghuatan (Dapingfang town, Chaoyang City, western Liaoning).

105 For the comparisons we present, the following taxa/specimens were analyzed first-hand (by XZ):
106 *Nurhachius ignaciobritoi* (both specimens, LPM 00023 and IVPP V-13288), *Liaoxipterus*
107 *brachyognathus* holotype (CAR-0018), *Hongshanopterus lacustris* holotype (IVPP V14582) and
108 *Haopterus gracilis* holotype (IVPP V11726). Data from other taxa was gathered from the
109 literature.

110 A phylogenetic analysis was performed based on the data matrix by Holgado *et al.* (2019) modified
111 with the inclusion of characters by Lü *et al.* (2008), Witton (2012), Andres *et al.* (2014), and new
112 characters; and the addition of the following taxa: *Archaeoistiodactylus linglongtaensis*,
113 *Kunpengopterus sinensis*, *Liaoxipterus brachyognathus* and *Nurhachius luei* sp. nov. (see SI). The
114 analysis was performed by TNT (Goloboff *et al.*, 2008) using the Traditional Search option, 10000
115 replicates, random seed = 0 and collapsing trees after search. The character and character states

116 list and the TNT file with the data matrix are available in the SI.

117 The electronic version of this article in Portable Document Format (PDF) will represent a
118 published work according to the International Commission on Zoological Nomenclature (ICZN),
119 and hence the new names contained in the electronic version are effectively published under that
120 Code from the electronic edition alone. This published work and the nomenclatural acts it contains
121 have been registered in ZooBank, the online registration system for the ICZN. The ZooBank
122 LSIDs (Life Science Identifiers) can be resolved and the associated information viewed through
123 any standard web browser by appending the LSID to the prefix <http://zoobank.org/>. The LSID for
124 this publication is: urn:lsid:zoobank.org:pub:03EF173E-4AB5-4C74-B80C-A6AAFA65E61C.
125 The online version of this work is archived and available from the following digital repositories:
126 PeerJ, PubMed Central and CLOCKSS.

127

128 **Results**

129 **Systematic Paleontology**

130 Pterosauria Kaup, 1834

131 Pterodactyloidea Plieninger, 1901

132 Istiodactylidae Howse *et al.*, 2001 (sensu Andres *et al.*, 2014)

133 *Nurhachius* Wang XL *et al.*, 2005

134 **Type species.** *Nurhachius ignaciobritoi* Wang XL *et al.*, 2005

135 **Synonym.** *Longchengpterus zhaoi* Wang L *et al.*, 2006

136 **Emended Diagnosis.** Istiodactylids that share the following features: slight dorsal deflection of
137 the palatal anterior tip; orbit piriform; craniomandibular joint located under the anterior margin of
138 the orbit; dentary symphysis about one third the length of the mandible; dentary symphysis with
139 gradual taper of the lateral margins; triangular, laterally compressed teeth lacking carinae; crowns
140 with both labial and lingual slight concavities; slight constriction between tooth crown and root.

141

142 *Nurhachius luei* sp. nov.

143 **ZooBank LSID for species.** urn:lsid:zoobank.org:act:6F93DC7F-20A7-4CBC-8A38-
144 1D6C802A1906.

145 **Etymology.** The specific name *luei* (/lyi/) honors the late Prof. Junchang Lü, who has made great
146 contributions to the study of Chinese pterosaurs.

147 **Holotype.** Skull, mandible and seven cervical vertebrae (BPMC-0204). The specimen is
148 permanently deposited and available for researchers at a public repository, the Beipiao Pterosaur
149 Museum of China, Beipiao, Liaoning Province, China (Fig. 1).

150 **Type Locality and Horizon.** Huanghuatan village, Dapingfang town, Chaoyang City, Liaoning
151 Province, China (Fig. 2); lower part of the Jiufotang Formation, Early Cretaceous (Aptian).

152

153 **Differential diagnosis.** The new species is diagnosed based on the following features: quadrate
154 inclined at 150°; medial process of the pterygoid broad and plate-like; dorsal median sulcus of the
155 mandibular symphysis extending up to the first pair of mandibular teeth; dorsally directed odontoid
156 (pseudotooth) of the mandibular symphysis, lacking a foramen on the lateral side and with a blunt
157 occlusal surface; ceratobranchial I of the hyoids accounting for 60% of mandibular length;
158 mandibular teeth extending distally beyond the symphysis.

159

160 **Description**

161 **Skull and mandible.** The skull is exposed in right lateral view, with some palatal elements that
162 are visible in dorsal view. The mandible is exposed in right dorsolateral view. The skull is 300 mm
163 long from the squamosal to the premaxillary tip (total skull length), and 74 mm high at its greatest
164 height, which is at the level of the occiput. The nasoantorbital fenestra is long, corresponding to
165 45% of the total skull length (premaxilla to squamosal) and 55% of the length from the
166 craniomandibular joint to the premaxilla. Anterior to the nasoantorbital fenestra, the long axis of
167 the rostrum is slightly deflected dorsally, as in other istiodactylids (Wang XL *et al.*, 2005; Andres
168 & Ji, 2006; Lü *et al.*, 2008; Witton, 2012), as well as *Ikrandraco avatar* and anhanguerians (e.g.
169 Kellner & Tomida, 2000; Wang XL *et al.*, 2014; 2015; Holgado *et al.*, 2019), but unlike
170 boreopterids (Lü & Ji, 2005; Lü, 2010; Jiang *et al.*, 2014). There is a strong palatal keel extending

171 from pre-narial part of the rostrum to the anterior third of the nasoantorbital fenestra. The
172 craniomandibular joint levels with the anterior margin of the orbit, similarly to both specimens of
173 *N. ignaciobrito* (see Fig. 3; both specimens, LPM 00023 and IVPP V-13288; see Wang XL *et al.*,
174 2005; Wang L *et al.*, 2006; Lü *et al.*, 2008), *Anhanguera* spp. (see Kellner & Tomida, 2000) and
175 *Linlongopterus jennyae* (see Rodrigues *et al.*, 2015), but unlike *Istiodactylus* spp., in which the
176 joint is located anterior to the orbit (see Andres & Ji, 2006; Witton, 2012), and *Ikrandraco avatar*
177 (see Wang XL *et al.*, 2015), *Hamipterus tianshanensis* (see Wang XL *et al.*, 2014) and
178 *Ludodactylus sibbicki* (Frey *et al.*, 2003), in which the joint is located under the middle of the orbit.
179 The orbit is piriform, with the narrowest part being ventral, and without a suborbital vacuity. This
180 is similar to the condition seen in the referred specimen of *N. ignaciobrito* and unlike the rounded
181 orbit of *Istiodactylus*, which has also a suborbital vacuity (see Andres & Ji, 2006; Lü *et al.*, 2008;
182 Witton, 2012). The infratemporal fenestra is elliptical and much smaller than the orbit. The
183 supratemporal fenestra is poorly preserved.

184 **Premaxilla and Maxilla.** The premaxilla is fused with the maxilla and the suture is obliterated,
185 thus the boundary between the two bones cannot be traced. Consequently, the premaxillary and
186 maxillary teeth count is unknown. There is no premaxillary crest, as in all other istiodactylids and
187 *Haopterus gracilis*. The rostral tip of the premaxilla exhibits a slight dorsal deflection of palatal
188 anterior tip (Fig. 4), as evidenced from the uplifted positions of the two anteriormost teeth. This is
189 similar to what has already been reported for *Cimoliopterus* and anhanguerians (see Rodrigues &
190 Kellner, 2013).

191 **Nasal and Lacrimal.** The nasal and lacrimal form the anterodorsal margin of the orbit and the
192 posterodorsal margin of the nasoantorbital fenestra. The anterior end of the nasolacrimal coincides
193 with the highest point of the nasoantorbital fenestra, as in both specimens of *N. ignaciobrito* and
194 also *Ikrandraco avatar* (Wang XL *et al.*, 2005; Wang L *et al.*, 2006; Andres & Ji, 2006; Lü *et al.*,
195 2008; Wang XL *et al.*, 2015), but unlike *Istiodactylus latidens* and most anhanguerians (e.g.,
196 *Anhanguera*, *Tropeognathus* and *Hamipterus*), except for *Ludodactylus sibbicki*, in which the
197 highest point is posterior to the anterior end of the nasolacrimal (Campos & Kellner, 1985;
198 Wellnhofer, 1987; Kellner & Tomida, 2000; Wang XL *et al.*, 2014; Frey *et al.*, 2003). A nasal
199 descending process cannot be seen in BPMC-0204, possibly because it is still covered by rock.
200 There are no traces of an orbital process of the lacrimal invading the orbit, but the posterior margin

201 of the lacrimal is slightly damaged and a small process similar to the one seen in the holotype of
202 *N. ignaciobrito* may have been present and got lost (see Wang XL *et al.*, 2005; Wang L *et al.*, 2006;
203 Andres & Ji, 2006; Lü *et al.*, 2008). The lacrimal contacts the lacrimal process of the jugal at about
204 the mid-height of the posterior margin of the nasoantorbital fenestra. The nasal is bordered dorsally
205 by the premaxilla and by the prefrontal posteroventrally.

206 **Jugal and Quadratojugal.** The jugal is partially preserved, missing part of the maxillary process
207 and the base of the lacrimal process. The jugal sends a postorbital process to contact the postorbital,
208 separating the orbit and the infratemporal fenestra. Posteriorly, the jugal contacts the
209 quadratojugal, which forms the anteroventral of the infratemporal fenestra.

210 **Quadrate.** Sutures at the lateral surface of the quadrate are unclear. It is unclear whether the
211 articulation with the mandible is helical or not. The mid-region of the quadrate is lost. The dorsal
212 portion of the quadrate contacts the quadratojugal anteriorly and the squamosal dorsally. The
213 quadrate is inclined backwards at an angle of 150° , unlike both specimens of *N. ignaciobrito* (Fig.
214 3), in which it slopes at $\sim 160^\circ$ ($160^\circ 4'$ in the holotype; Wang XL *et al.*, 2005; 163° in the referred
215 specimen; Wang L *et al.*, 2006).

216 **Prefrontal.** The prefrontal is a small bone that forms the anterodorsal margin of the orbit,
217 contacting the nasolacrimal. A suture between these two bones can be seen anteroventrally. The
218 dorsoposterior tip of this bone contacts the frontal.

219 **Frontal.** The frontal seems to be fused with the premaxilla and parietal, with no visible sutures. It
220 is unclear whether the posterodorsal extension of the frontal forms a blunt and low frontoparietal
221 crest as in *Anhanguera* (see Kellner & Tomida, 2000) or not.

222 **Parietal and Squamosal.** The parietal and squamosal are poorly preserved, especially the latter.
223 The squamosal outline cannot be properly identified. The parietal preserves a shallow depression
224 in its surface that corresponds to the medial wall of the supratemporal fenestra. The dorsal limits
225 of this fossa level with the orbit and extend ventrally to the region of contact between the squamosal
226 and the postorbital.

227 **Postorbital.** The postorbital is slender and does not exhibit a triangular shape, oppositely to the
228 triangular condition that is seen in anhanguerids (e.g. Kellner & Tomida, 2000). Instead, it is like
229 a three-pointed star (= concave equilateral hexagon) as in *Haopterus gracilis* (see Wang XL & Lü,

230 2001); that is, is essentially composed of three connected processes. The anterior region of the
231 postorbital which is formed by the frontal and jugal processes, is arched and forms the posterior
232 margin of the orbit. The squamosal process is shorter than the other processes and separates the
233 supra and infratemporal fenestrae. There is no orbital process of the postorbital invading the orbit,
234 unlike *Istiodactylus* (Andres & Ji, 2006; Witton, 2012).

235 **Palatal elements.** Due to crushing, some palatal elements are visible in dorsal view, though few
236 details can be observed. The vomers form a long, slender bony bar that separates the choanae, as
237 in *Hongshanopterus lacustris* (see Wang XL *et al.*, 2008a). Of the pterygoid, only the medial
238 process can be seen. It is large and plate-like as that of *Hongshanopterus lacustris* (see Wang XL
239 *et al.*, 2008a) and, to a lesser extent, the anhanguerids, in which the process is also broad but less
240 medially expanded (e.g., Campos & Kellner, 1985; Frey *et al.*, 2003). This differs from the slender
241 medial processes of the pterygoid of azhdarchoids (e.g., Pinheiro & Schultz, 2012; Kellner, 2013;
242 Pêgas *et al.*, 2018) or those of the referred specimen of *N. ignaciobritoi* (see Wang L *et al.*, 2006;
243 Lü *et al.*, 2008) and *Ikrandraco avatar* (see Wang XL *et al.*, 2015).

244 **Dentary.** The dentaries are fused rostrally forming a symphysis that accounts for 36% of total
245 mandibular length, which is 240 mm long. The dorsal surface of the symphysis presents a deep
246 and broad median sulcus that extends anteriorly up to the level of the first pair of teeth (Fig. 5).
247 The rostral tip of the dentary symphysis has an odontoid (pseudotooth), that is located between the
248 first pair of teeth, is smaller than the adjacent tooth crowns and is dorsally directed. The odontoid
249 lacks the neurovascular foramen piercing its surface in the referred specimen of *N. ignaciobritoi*
250 (see Wang L *et al.*, 2006). The odontoid has the same orientation as that of *Istiodactylus latidens*
251 (see Witton, 2012; Martill, 2014) and *Lonchodraco giganteus* (see Rodrigues & Kellner, 2013, fig.
252 4E-F), unlike the sub-horizontal odontoids of both specimens of *N. ignaciobritoi* (see Wang XL *et*
253 *al.*, 2005; Wang L *et al.*, 2006) and *Ikrandraco avatar* (see Wang XL *et al.*, 2015). The symphysis
254 presents 11 tooth positions per side.

255 **Surangular, Articular and Angular.** The lateral surface of the posterior region of the right
256 mandibular ramus is composed by the surangular, angular and articular. A suture separates the long
257 anterior process of the surangular from the dentary dorsally. Posteriorly, the surangular becomes
258 deeper and is sutured with the angular. The boundary between the angular and the dentary,
259 however, cannot be distinguished, nor the boundary between the angular and the articular. The

260 articular forms the posterior part of the mandible, including the articular surface for the quadrate
261 and the retroarticular process, which is pointed, dorsoventrally low and distally tapering.

262 **Hyoid.** Only the right ceratobranchial I is exposed along the ventral margin of the right mandibular
263 ramus (Fig. 1). A small portion of the posterior part is missing. The ceratobranchial I is a long rod-
264 like bone extending along the whole length of the mandibular rami.

265 **Dentition.** There are 12 tooth positions along the right side of the upper jaw and 11 tooth positions
266 along each side of the lower jaw, with an inferred total count of 46 tooth positions. The first two
267 teeth of the upper jaw (which are presumably premaxillary teeth) are procumbent. The first tooth
268 forms an angle of 130° with the main axis of the rostrum, while the second forms an angle of 123° .
269 The third tooth is also slightly procumbent, forming an angle of 100° with the palatal plane. All
270 subsequent teeth are perpendicular to the main axis of the rostrum. The first two dentary teeth are
271 also slightly procumbent. The last two alveoli of the right maxilla are empty, and the last one is
272 placed just anterior to the level of the rostral end of the nasoantorbital fenestra. All of the crowns
273 are triangular in labiolingual view and labiolingually compressed, as typical of the Istiodactylidae.
274 The base of the crowns is mesiodistally inflated. The lingual surface of the crown is concave with
275 a well-marked basoapical depression and a low transversal convexity at the base, that forms a
276 lingual cingulum. The labial surface is mostly convex with a shallow concavity in the middle of
277 the basal part of the crown. No carinae are present along the mesial and distal cutting margins of
278 the crowns. The same features occur in the crowns of the holotype of *N. ignaciobrito*. The teeth
279 exhibit a slight constriction between crown and root (Fig. 5). This feature is also shared with *N.*
280 *ignaciobrito* (see Wang XL *et al.*, 2005).

281 The first nine pairs of teeth of the upper jaw are large and subequal in size. Their apicobasal total
282 length of their crowns is about 12 mm and the crown apicobasal length is about 7 mm, and the
283 mesiodistal width of the socket is 4 mm. The smallest crown is 6 mm in apicobasal length and 2
284 mm in mesiodistal width.

285 *N. luei* sp. nov. also presents an interesting pattern of tooth replacement. Two teeth occur in the
286 tenth alveolus of the right dentary: a large functional one and a not yet fully erupted replacement
287 tooth. The replacement tooth was erupting anterolabially to the functional tooth, instead of
288 posterolingually as reported in other pterodactyloid pterosaurs like *Anhanguera* (see Kellner &
289 Tomida, 2000; Fastnacht, 2001) and '*Cearadactylus*' *ligabuei* (see Dalla Vecchia, 1993).

290 **Cervical vertebrae.** Seven cervical vertebrae are preserved, including the atlas-axis complex
291 (although the atlas itself cannot be identified). They are articulated, except for the 7th vertebra,
292 which is disarticulated but still contacting the 6th vertebra. The 3rd cervical, with 38.4 mm, is
293 longer than the 4th through 7th cervicals which are of similar length. The neural spine is damaged
294 in most cervicals, except that of the 4th vertebra, which is high and with a peculiar shape (its
295 anterior margin is anteriorly inclined). The apex of the neural spine is gently rounded. The
296 postzygapophyses are posterodorsally oriented. The centrum extends posterior to the
297 postzygapophyses. In the 3rd to the 7th cervicals, a large pneumatic foramen can be seen on the
298 posterior half of the centrum below the neural arch.

299 **Phylogenetic analysis results**

300 The phylogenetic analysis by parsimony produced 51 most parsimonious trees with a minimum
301 length of 360 steps, with minimum consistency index of 0.642 and retention index of 0.862. As
302 suspected by Witton (2012), *Hongshanopterus lacustris* and *Haopterus gracilis* were found to be
303 closely related to the Istiodactylidae in the strict consensus tree (Fig. 6), but they fall outside them.
304 The Istiodactylidae have been defined by Andres *et al.* (2014) as the least inclusive clade
305 containing *Istiodactylus latidens* Seeley 1901 and *Nurhachius ignaciobritoi* Wang XL *et al.* 2005.
306 In the strict consensus tree (Fig. 6), the Istiodactylidae contain *Nurhachius*, *Liaoxipterus*
307 *brachyognathus* and *Istiodactylus*. *N. ignaciobritoi* and *N. luei* sp. nov. were recovered as sister
308 taxa. *Istiodactylus latidens* and *I. sinensis* were also recovered as sister taxa and *Liaoxipterus*
309 *brachyognathus* is the sister-taxon of *Istiodactylus*.

310 *Istiodactylus* has the following five synapomorphies: presence of a suborbital opening (character
311 11, state 1); prenarial portion of the rostrum less than 20% the skull length (character 25, state 0);
312 presence of an orbital process in the jugal (character 56, state 1); and sharp carinae in the teeth
313 (character 96, state 1). *Istiodactylus* shares with *Liaoxipterus brachyognathus* the following
314 synapomorphies: subparallel lateral margins of the jaws (character 24, state 1); mandibular
315 symphysis shorter than 33% of the mandible length (character 78, state 1); and rounded outline of
316 the rostral end of the mandible (character 79, state 0).

317 The genus *Nurhachius* is characterized by the following five synapomorphies: piriform orbit
318 (character 7, state 2); cranio-mandibular articulation-under the anterior margin of orbit (character

319 58, state 2); dorsal deflection of the palatal anterior tip (character 71, state 1); teeth crowns with
320 labial and lingual depressions (character 100, state 1); teeth with a mesiodistal constriction
321 between crown and root (character 101, state 1). The presence of a dorsal deflection of the palatal
322 anterior tip represents a homoplasy with *Anhangueria* + *Cimoliopterus*.

323 The Istiodactylidae share the following seven synapomorphies: ventral margin of the
324 nasoantorbital fenestra longer than 40% of skull length (character 4, state 1); orbit reaching high
325 in the skull, with the dorsal margin surpassing the dorsal margin of the nasoantorbital fenestra
326 (character 10, state 1); skull height (exclusive of cranial crests) over 25% of the jaw length
327 (character 23, state 1); lacrimal process of jugal inclined posteriorly (character 54, state 2); helical
328 jaw-joint absent (character 59, state 0); palatal occlusal surface: strong palatal ridge confined to
329 the posterior portion of the palate (character 71, state 3); teeth confined to about the anterior third
330 of the jaws (character 86, state 3).

331 *Hongshanopterus lacustris* results to be the sister-taxon of the Istiodactylidae. The clade
332 *Hongshanopterus lacustris* + Istiodactylidae presents two synapomorphies: tooth crowns strongly
333 compressed laterally (character 95, state 2); and mesial crowns under twice as long as wide
334 (character 97, state 0).

335 *Haopterus gracilis* results as the sister-taxon of *Hongshanopterus lacustris* + Istiodactylidae,
336 sharing teeth that are confined to the anterior half of the jaws (character 86, state 2).

337 The Istiodactylidae, *Hongshanopterus lacustris* and *Haopterus gracilis* share with *Ikrandraco*
338 *avatar* four synapomorphies: narrow lacrimal process of jugal (character 53, state 1); quadrate
339 inclination relative to the ventral margin of the skull is 150° or more (character 57, state 3); tooth
340 crowns slightly compressed laterally (character 95, state 2); lingual cingulum present at the base
341 of tooth crown (character 102, state 1). The last two character states are also shared with
342 *Lonchodraco giganteus*.

343 Bremer support values were 1 for the genus *Istiodactylus*, 3 for *Istiodactylus* + *Liaoxipterus*, 5 for
344 the genus *Nurhachius*, 3 for Istiodactylidae, 3 for *Hongshanopterus* + Istiodactylidae, 1 for
345 *Haopterus* + (*Hongshanopterus* + Istiodactylidae), 1 for *Ikrandraco* + *Lonchodraco* and 2 for the
346 clade that joins all of these taxa.

347

348 **Discussion**

349 For over a century, *Istiodactylus latidens* was the only known istiodactylid (Witton, 2012). In the
350 last 15 years, three new istiodactylids have been reported from the Jiufotang Formation of China:
351 *N. ignaciobritoi* (described in 2005); *Istiodactylus sinensis* and *Longchengpterus zhaoi* (both
352 described in 2006); and *Liaoxipterus brachyognathus* (originally described in 2005 as a purported
353 ctenochasmatid and referred to the Istiodactylidae in 2008; Dong & Lü, 2005; Wang XL *et al.*,
354 2005; Wang L *et al.*, 2006; Andres & Ji, 2006; Lü *et al.*, 2008). However, the validity of some of
355 them is debated. According to Lü *et al.* (2008), the holotypes of *Longchengpterus zhaoi* and *N.*
356 *ignaciobritoi* are indistinguishable, sharing general skull shape and tooth morphology. Therefore,
357 *Longchengpterus zhaoi* was considered a junior synonym of *N. ignaciobritoi* by Lü *et al.* (2008).
358 Witton (2012) provisionally considered both of them as valid and distinct taxa, coding them
359 separately in his phylogenetic analysis though without discussing it further. They were coded
360 differently as for tooth count and spacing, with *Nurhachius* that was considered to have more
361 numerous and more spaced teeth. However, both specimens exhibit a similar number of upper
362 teeth (13 pairs in the holotype of *N. ignaciobritoi* and 12 pairs in *L. zhaoi*) and similar spacing
363 (Wang XL *et al.*, 2005; Lü *et al.*, 2008). Furthermore, the holotypes and only specimens of
364 *Longchengpterus zhaoi* and *N. ignaciobritoi* share further features that are unique within
365 istiodactylids (Fig. 3): the high quadrate inclination ($\sim 160^\circ$), the reduced medial process of the
366 pterygoid, the upper dentition ending at the level of the nasoantorbital fenestra, and the sub-
367 horizontal odontoid in the mandibular symphysis. Therefore, we follow Lü *et al.* (2008) in
368 considering *Longchengpterus zhaoi* as a junior synonym of *N. ignaciobritoi*.

369 *N. luei* sp. nov. is an istiodactylid based on the following features: nasoantorbital fenestra longer
370 than 40% of skull length, dentary symphysis less than 33% of mandible length; and triangular,
371 labiolingually compressed tooth crowns. It shares with *N. ignaciobritoi* a piriform orbit, a dorsally
372 deflected palatal anterior tip, a cranio-mandibular articulation positioned under the anterior margin
373 of the orbit (Fig. 3), tooth crowns with labial and lingual depressions, and teeth with mesiodistal
374 constrictions between crown and root (Fig. 5; 6). All these features are present in the holotype of
375 *N. ignaciobritoi*, while in the referred specimen the dorsal deflection of the palatal anterior tip

376 cannot be assessed as the rostrum tip is missing. Concerning the crown, with both a labial and a
377 lingual depression, we note that this morphology is reflected in the shape of the alveoli in *N.*
378 *ignaciobritoi*, with concave labial and lingual margins (Fig. 5). The dorsal deflection of the palatal
379 anterior tip is present in the rostral tip of the skull of the holotype of *N. ignaciobritoi*, as evidenced
380 from the dorsal position of the first pair of alveoli, (see Fig. 4C-D), although it was not mentioned
381 in the original description (Wang XL *et al.*, 2005), as well as in the holotype of *N. luei*. This
382 character was utilized in a data matrix for the first time by Rodrigues & Kellner (2013), and
383 resulted to be a synapomorphy of Anhangueria + *Cimoliopterus*. According to our phylogenetic
384 analysis (Fig. 7), this feature was independently acquired by *Nurhachius* and Anhangueria +
385 *Cimoliopterus*.

386 *N. luei* sp. nov. differs from *N. ignaciobritoi* in the following features: the quadrate is inclined at
387 150° instead of the $\sim 160^\circ$ of *N. ignaciobritoi*; the medial process of the pterygoid is broad and
388 plate-like, whereas it is reduced in *N. ignaciobritoi* (see Fig. 3); the dorsal median sulcus of the
389 mandibular symphysis extends up to the first pair of teeth, whereas it reaches the sixth pair of teeth
390 in *N. ignaciobritoi* (see Fig. 5); the odontoid (pseudotooth) lacks a lateral foramen, whereas a
391 foramen is present in the referred specimen of *N. ignaciobritoi* (see Martill, 2014, fig. 7C-D); the
392 odontoid has a blunt occlusal surface, whereas the surface is sharp in *N. ignaciobritoi* (Fig. 5); the
393 odontoid is dorsally directed, whereas it is anterodorsally directed in *N. ignaciobritoi* (but see
394 Martill, 2014, p. 57, right column, lines 21-23); and the ceratobranchial I of the hyoid apparatus
395 accounts for 60% of the mandibular length, whereas it accounts for 35% of the mandibular length
396 in *N. ignaciobritoi* (Fig. 5).

397 Concerning quadrate inclination, we do not regard this variation as intraspecific as the variation
398 does not surpass 3° in the archaeopterodactyloid *Pterodactylus antiquus* (specimens BSPG AS I
399 739, BSPG 1929 I 18, BMMS 7; see Bennett, 2013; Vidovic & Martill, 2014), 3° in the
400 anhanguerian *Hamipterus tianshanensis* (IVPP V18931.1, holotype, and IVPP V18935.1,
401 paratype; see Wang XL *et al.*, 2014), 5° in *Aerodactylus scolopaciceps* (BSPG 1883 XVI 1, BSPG
402 1937 I 18, BSPG AS V 29 a/b; see Vidovic & Martill, 2014), and is less than 6° in *Pteranodon*
403 *longiceps* (specimens YPM 1177, USNM 13656, KUVV 2212, KUVV 27821) and also in
404 *Pteranodon sternbergi* (specimens FHSM VP 339, YPM 1179, UALVP 24238; see Bennett, 1994;
405 2001). Quadrate inclination has indeed been regarded as diagnostic before for tapejarids (Kellner,

406 2013) and *Pteranodon* (Bennett, 1994). We regard this feature as potentially diagnostic at least
407 until further specimens of each species of *Nurhachius* are found.

408 Both specimens of *N. ignaciobritoi* come from the upper part of the Jiufotang Formation (see Wu
409 *et al.*, 2018), while the holotype of *N. luei* comes from the lowermost part of the Jiufotang
410 Formation. This stratigraphic distribution might be suggestive of an anagenetic link between the
411 two species, similar to the case of *Pteranodon longiceps* (from the upper Smoky Hill Chalk) and
412 *Pteranodon sternbergi* (from the lower Smoky Hill Chalk) according to Bennett (1994), but see
413 taxonomic controversies (Kellner, 2010; 2017; Martin-Silverstone *et al.*, 2017; Acorn *et al.*, 2017).
414 The same has been speculated as a possible explanation for the occurrence of multiple species of
415 *Anhanguera* (Pinheiro & Rodrigues, 2017), *Thalassodromeus* and *Tupuxuara* (Pêgas *et al.*, 2018)
416 in the Romualdo Formation. However, these cases still lack stratigraphic control for support, and
417 the time resolution of the Romualdo Formation is still in question (see Pinheiro & Rodrigues,
418 2017).

419 Wang XL *et al.* (2008a) were unable to differentiate *Liaopterus brachyognathus* from
420 *Longchengpterus zhaoi*, and suggested that *Longchengpterus zhaoi* could be a junior synonym of
421 *Liaopterus brachyognathus*. However, as observed by Lü *et al.* (2008), the rostral end of the
422 mandibular symphysis is rounded in *Liaopterus brachyognathus* (in dorsal view, as it is in
423 *Istiodactylus latidens*), whereas it is triangular in “*Longchengpterus zhaoi*”. Furthermore, as coded
424 by Andres *et al.* (2014), both jaws show an attenuated taper (in occlusal view) in *Longchengpterus*
425 *zhaoi*, while the lateral margins of the lower jaw are sub-parallel in *Liaopterus brachyognathus*
426 (Fig. 8A) as in *Istiodactylus latidens*. Additionally, the mandibular symphysis of *Liaopterus*
427 *brachyognathus* is relatively stouter than that of *Longchengpterus zhaoi*: their length/width ratios
428 are 0.43 and 0.27, respectively. It is worthy of being noticed that the mandibular symphysis of
429 *Longchengpterus zhaoi* is incorrectly drawn in Martill (2014, fig. 7B), as resulting to be much
430 shorter than it is. The actual configuration can be clearly assessed in the description by Lü *et al.*
431 (2008) and in Fig. 5A. We thus follow Lü *et al.* (2008) and Witton (2012) in considering
432 *Liaopterus brachyognathus* as distinct from *Longchengpterus zhaoi*, which we consider as a
433 junior synonym of *N. ignaciobritoi*.

434 Lü *et al.* (2008) and Witton (2012) noticed that comparison between *Liaopterus brachyognathus*

435 and *Istiodactylus sinensis* is very limited because the former is represented by a mandible exposed
436 in occlusal view, while the latter is a partial skeleton including a mandible exposed in lateral view.
437 However, *Liaopterus brachyognathus* differs from *Istiodactylus* in the lack of mesial carinae,
438 according to Lü *et al.* (2008) and the dataset of Andres *et al.* (2014). We thus follow these authors
439 in considering *Liaopterus brachyognathus* as a valid taxon.

440 According to our phylogenetic analysis, *Istiodactylus* is monophyletic, comprising *I. latidens* and
441 *I. sinensis*. *Liaopterus brachyognathus* is the sister-taxon of *Istiodactylus*, and *Nurhachius* is the
442 sister-taxon of *Liaopterus brachyognathus* + *Istiodactylus*, in agreement with the results of the
443 phylogenetic hypothesis published by Longrich *et al.* (2018). In our analysis, *N. luei* results to be
444 the sister-taxon of *N. ignaciobritoi*, supporting their congeneric status. The relationships within
445 the Istiodactylidae obtained in our analysis are similar to those found by Andres *et al.* (2014), but
446 *Longchengpterus zhaoi* is not the sister-taxon of *N. ignaciobritoi* in the cladogram of figure S2 of
447 Andres *et al.* (2014).

448 *Haopterus gracilis* was first described by Wang XL & Lü (2001) and referred to the
449 Pterodactylidae. However, it resulted to be close to *Istiodactylus latidens* in the 50% majority-rule
450 tree by Lü *et al.* (2008) and formed a polytomy with *Nurhachius* and *Istiodactylus* in the strict
451 consensus tree by Lü *et al.* (2009). *Hongshanopterus lacustris* was described by Wang XL *et al.*
452 (2008a) and interpreted as a primitive istiodactylid. In the strict consensus tree by Witton (2012),
453 the Istiodactylidae include *Nurhachius ignaciobritoi*, *Longchengpterus zhaoi*, *Istiodactylus*
454 *latidens*, *Istiodactylus sinensis*, and *Liaopterus brachyognathus*. *Haopterus gracilis* and
455 *Hongshanopterus lacustris* form a polytomy with *Pteranodon longiceps*, *Coloborhynchus*
456 *spielbergi* and the Istiodactylidae (Witton, 2012).

457 In the phylogenetic analysis of Andres *et al.* (2014; fig. S2), *Haopterus gracilis* results to be a
458 basal eupterodactyloidean and *Hongshanopterus* a basal ornithocheiromorph. Recently, Holgado
459 *et al.* (2019) have published a phylogenetic hypothesis in which *Hongshanopterus lacustris* would
460 be the sister-group of the Istiodactylidae (although it is erroneously reported within this clade as
461 the basal member in their fig. 5A), while *Haopterus gracilis* would be closer to anhanguerians than
462 to istiodactylids (see Holgado *et al.*, 2019).

463 In our analysis, *Haopterus gracilis* and *Hongshanopterus lacustris* are closely related to the

464 Istiodactylidae, as found by Lü *et al.* (2008) and Wang XL *et al.* (2008a), respectively.
465 *Hongshanopterus lacustris* results to be the sister-taxon of the Istiodactylidae, as in the analysis
466 by Holgado *et al.* (2019). *Hongshanopterus lacustris* shares with the istiodactylids the presence of
467 labiolingually compressed teeth with triangular crowns. *Haopterus gracilis* results to be the sister-
468 taxon of *Hongshanopterus lacustris* + Istiodactylidae, a relationship that is supported by the
469 possession of a dentition restricted to the anterior half of the jaws.

470 *Haopterus*, *Hongshanopterus* and istiodactylids share also the presence of a lingual cingulum in
471 the tooth crown, a feature that occurs also in *Ikrandraco avatar*. A lingual cingulum can be seen
472 in *Nurhachius luei* and *N. ignaciobrito* (Fig. 6). The same feature has been previously reported
473 for *Liaoxipterus brachyognathus* (see Lü *et al.*, 2008) and depicted for *Ikrandraco avatar* (see the
474 second figure of Wang XL *et al.*, 2015). In *Haopterus gracilis*, the labiodistal view of the third
475 right upper tooth presents a lingually oriented convexity that also suggests the presence of this
476 feature (Fig. 8).

477 *Ikrandraco avatar* shares with istiodactylids also a narrow lacrimal process of the jugal and a
478 quadrate inclined at 150° or over (the inclination of the quadrate is unknown in *Haopterus gracilis*
479 and *Hongshanopterus lacustris*). *Ikrandraco avatar* and *Haopterus gracilis* also exhibit a certain
480 degree of labiolingual compression of the teeth, at least in the distal part of the dentition (Wang
481 XL & Lü, 2001; Wang XL *et al.*, 2015), though not to the same degree seen in the istiodactylids
482 and *Hongshanopterus*. The last two mandibular alveoli preserved in the holotype of *Lonchodraco*
483 *giganteus* (the sister-taxon of *Ikrandraco avatar* in our analysis) are also labiolingually narrow
484 (see Martill, 2011; Rodrigues & Kellner, 2013).

485 Furthermore, *Ikrandraco avatar* and *Lonchodraco giganteus* also share with istiodactylids the
486 presence of an odontoid, which is anterodorsally oriented in the former and dorsally oriented in
487 the latter (see Rodrigues & Kellner, 2013; Wang XL *et al.*, 2015).

488 A close relationship among *Ikrandraco avatar*, *Lonchodraco giganteus* and istiodactylids is found
489 here for the first time. *Ikrandraco avatar* formed a polytomy with the Istiodactylidae,
490 *Cimoliopterus* and the Anhangueria in the phylogenetic analysis by Wang XL *et al.* (2015) and
491 *Lonchodraco giganteus* is outside the Lanceodontia in the phylogenetic analysis by Longrich *et*
492 *al.* (2018).

493 *Archaeoistiodactylus linglongtaensis* is based on the sole holotype (JPM04-0008), including
494 fragments of skull and one displaced maxillary tooth, a partial lower jaw in occlusal view with two
495 teeth in place, an almost complete forelimb, a femur and a tibia. It is from the Middle Jurassic
496 (Bathonian-Oxfordian) Tiaojishan Formation. *A. linglongtaensis* was described by Lü & Fucha
497 (2010) who interpreted it as the "ancestor form of the known istiodactylid pterosaur [sic]" (Lü &
498 Fucha, 2010, p. 113). Lü & Fucha (2010) observed that JPM04-0008 and the istiodactylids share
499 teeth with triangular crowns and an odontoid (pseudotooth) on the mandibular symphysis. That
500 odontoid was mistaken for a mid-line, unpaired tooth by Sullivan *et al.* (2014), but it had been
501 explicitly described as a bony process by Lü & Fucha (2010, p. 116). Lü & Fucha (2010) also
502 observed that the single maxillary tooth is recurved as in *Hongshanopterus lacustris*, and reported
503 the presence of a warped deltopectoral crest in the humerus, which is a diagnostic feature of the
504 Pteranodontoidea (Kellner, 2003). They noted that *A. linglongtaensis* differs from istiodactylids
505 and all other pterodactyloids in the relatively short fourth metacarpal and in the presence of tibia,
506 and second and third phalanges of the wing digit with subequal lengths. If actually a
507 pterodactyloid, it would represent one of the oldest occurrences of the Pterodactyloidea, being
508 coeval or even older than the Callovian-Oxfordian basalmost pterodactyloid *Kryptodrakon*
509 *progenitor* (see Andres *et al.*, 2014).

510 Its identification as a pterodactyloid was disputed by Martill & Etches (2013), who affirmed that
511 JPM04-0008 is probably a badly preserved specimen of *Darwinopterus*, though they did not
512 present any evidence to support this statement. According to Sullivan *et al.* (2014), the short fourth-
513 metacarpal, the long humerus and short first wing phalanx are typical of non-pterodactyloid
514 pterosaurs (see Kellner, 2003; Unwin, 2003; Andres *et al.*, 2010), thus JPM04-0008 is not a
515 pterodactyloid. These features united to the presence of a confluent nasoantorbital fenestra in
516 JPM04-0008, led Sullivan *et al.* (2014) to interpret *A. linglongtaensis* as a basal monofenestratan.

517 However, *A. linglongtaensis* has never been included in any phylogenetic analysis to test its basal
518 monofenestratan affinity, thus it was included in the analysis performed in this paper. Our results
519 (Fig. 6) confirm the interpretation by Sullivan *et al.* (2014). *Archaeoistiodactylus linglongtaensis*
520 lacks the following pterodactyloid features: humerus length under 1.5 times metacarpal IV length;
521 ulna under double the length of metacarpal IV; and femur subequal to or shorter than metacarpal
522 IV. The humerus of JPM04-0008 is crushed and the original orientation of the deltopectoral crest

523 cannot be assessed. Differently from pterodactyls, the deltopectoral crest of JPM04-0008 is
524 confined to the proximal region of the humerus (Wang XL *et al.*, 2009). *A. linglongtaensis* also
525 lacks pneumatic foramina on the centra of the mid-cervical vertebrae, which is a diagnostic feature
526 of the Dsungaripteroidea (the least inclusive clade containing *Nyctosaurus* and *Quetzalcoatlus*,
527 which includes also the Istiodactylidae; Kellner, 2003; Andres *et al.*, 2014). Furthermore, *A.*
528 *linglongtaensis* exhibits low neural spines, like wukongopterids (see Wang XL *et al.* 2009; 2010;
529 Lü *et al.*, 2009; 2011; Cheng *et al.*, 2017) and unlike istiodactylids (see Wang L *et al.*, 2006; Lü
530 *et al.*, 2008).

531 The dentition of *A. linglongtaensis* is indeed reminiscent of that of the Istiodactylidae due to the
532 short triangular aspect of the crowns in labiolingual view. However, this feature is also present in
533 the wukongopterids *Wukongopterus lii*, *Darwinopterus robustodens*, *Darwinopterus*
534 *linglongtaensis* and *Kunpengopterus sinensis*, though not in *Darwinopterus modularis* (see Wang
535 XL *et al.* 2009; 2010; Lü *et al.*, 2009; 2011; Cheng *et al.*, 2017). Furthermore, in *A. linglongtaensis*
536 the alveoli are circular (Lü & Fucha, 2010), as in wukongopterids, not labiolingually compressed
537 triangular teeth as in istiodactylids. The presence or absence of an odontoid in the lower jaw cannot
538 be confidently assessed in *Wukongopterus* and *Darwinopterus*, but can be seen in a specimen
539 referred to *Kunpengopterus sinensis* (see Cheng *et al.*, 2017), in convergence with the
540 istiodactylids. Finally, *A. linglongtaensis* shares with *Darwinopterus* and *Kunpengopterus*, but not
541 with *Wukongopterus*, the subequal in length second and third phalanges of the wing digit. Thus,
542 *A. linglongtaensis* may be closely related to *Darwinopterus* or *Kunpengopterus*. In our analysis,
543 *A. linglongtaensis* falls in a polytomy with *Darwinopterus linglongtaensis*, *D. robustodens* and
544 *Kunpengopterus sinensis* (Fig. 6). However, we were unable to access the specimen first-hand and
545 further scrutiny is desirable in order to confirm or deny this affinity.

546

547 **Conclusions**

548 The new specimen here described represents the second species for the genus *Nurhachius*,
549 previously restricted to its type-species *N. ignaciobrito*. A slight dorsal deflection of the palatal
550 anterior tip revealed to be a synapomorphy of *N. ignaciobrito* and *N. luei*. That feature was
551 previously thought to be restricted to the Anhangueria and *Cimoliopterus*. Unlike other

552 pterodactyls, the holotype of *N. luei* sp. nov. shows an anterolabial tooth replacement. The
553 position of *Hongshanopterus lacustris* and *Haopterus gracilis* as close taxa to the Istiodactylids is
554 supported by the performed phylogenetic analysis. *Ikrandraco avatar* and *Lonchodraco giganteus*
555 resulted to be sister taxa, and closer to istiodactylids than to other lanceodontians. The
556 phylogenetic analysis supports the reinterpretation of *Archaeoistiodactylus linglongtaensis* as a
557 non-pterodactylid monofenestratan, probably a wukongopterid.

558

559 **Acknowledgements**

560 We thank Shu'an Ji and Xuefang Wei (IG-CAGS, Institute of Geology, Chinese Academy of
561 Geological Sciences) for the help all along. Thanks to Cunyu Liu (BPMC, Beipiao Pterosaur
562 Museum of China), Dongyu Hu (SNU, Shenyang Normal University), Xiaolin Wang & Shunxing
563 Jiang (IVPP, Institute of Vertebrate Paleontology and Paleoanthropology) for access to specimens
564 under their care. RVP thanks Kamila Bandeira, Lucy Souza and Natan Brilhante (Museu
565 Nacional/UFRJ) for technical help with image software. We thank Zoological Museum (SNM),
566 Copenhagen University for hospitality during X. Y. Zhou's and R. V. Pêgas' stay in Copenhagen
567 with access to important pterosaur specimens, and for M. E. C. Leal's status as guest researcher,
568 and N. Bonde's work space as emeritus (and Senior Scientist, Fur Museum). Thanks to Fabio M.
569 Dalla Vecchia, Felipe Pinheiro, Chris Bennett and an anonymous reviewer for their thoughtful and
570 constructive critiques; and to editor Graciela Piñeiro for her kind attention.

571

572 **References**

- 573 **Acorn JH, Martin-Silverstone E, Glasier JRN, Mohr S, Currie PJ. 2017.** Response to Kellner
574 (2017) 'Rebuttal of Martin-Silverstone, E., JRN Glasier, JH Acorn, S. Mohr, and PJ Currie,
575 2017'. *Vertebrate Anatomy Morphology Palaeontology* **3**: 90-92.
- 576 **Andres B, Ji Q. 2006.** A new species of *Istiodactylus* (Pterosauria, Pterodactyloidea) from the
577 Lower Cretaceous of Liaoning, China. *Journal of Vertebrate Paleontology* **26(1)**: 70-78.
- 578 **Andres B, Clark JM, Xu X. 2010.** A new rhamphorhynchid pterosaur from the Upper Jurassic of
579 Xinjiang, China, and the phylogenetic relationships of basal pterosaurs. *Journal of Vertebrate*
580 *Paleontology* **30(1)**: 163-187.
- 581 **Andres B, Clark JM, Xu X. 2014.** The earliest pterodactylid and the origin of the group. *Current*

- 582 Biology **24(9)**: 1011-1016.
- 583 **Bennett SC. 1994.** Taxonomy and systematics of the Late Cretaceous pterosaur *Pteranodon*
584 (Pterosauria, Pterodactyloidea). *Occasional papers of the Natural History*
585 *Museum/The University of Kansas* (169):1–70.
- 586 **Bennett SC. 2001.** The osteology and functional morphology of the Late Cretaceous pterosaur
587 Pteranodon Part I. General description of osteology. *Palaeontographica Abteilung A* **2001**:
588 1–112.
- 589 **Bennett SC. 2013.** New information on body size and cranial display structures of *Pterodactylus*
590 *antiquus*, with a revision of the genus. *Paläontologische Zeitschrift* **87(2)**: 269–289.
- 591 **Campos DA, Kellner AWA. 1985.** Panorama of the flying reptiles study in Brazil and South
592 America. *Anais da Academia Brasileira de Ciências* **57**: 453–466.
- 593 **Chang MM, Chen PJ, Wang YQ, Wang Y, Miao DS. eds. 2003.** *The Jehol Biota*. Shanghai Sci.
594 & Tech. Publ. 208 pp.
- 595 **Chang SC, Zhang HC, Renne PR, Fang Y. 2009.** High-precision ⁴⁰Ar/³⁹Ar age for the Jehol
596 Biota. *Palaeogeography, Palaeoclimatology, Palaeoecology* **280**: 94–104.
- 597 **Cheng X, Jiang SX, Wang XL, Kellner AWA. 2017.** Premaxillary crest variation within the
598 Wukongopteridae (Reptilia, Pterosauria) and comments on cranial structures in
599 pterosaurs. *Anais da Academia Brasileira de Ciências* **89(1)**: 119-130.
- 600 **Dalla Vecchia FM. 1993.** *Cearadactylus? ligabuei*, nov. sp., a new Early Cretaceous (Aptian)
601 pterosaur from Chapada do Araripe (Northeastern Brazil). *Bolletino della Societa*
602 *Paleontologica Italiana* **32**: 401–409.
- 603 **Dong ZM, Lü JC. 2005.** A new ctenochasmatid pterosaur from the Early Cretaceous of Liaoning
604 Province. *Acta Geologica Sinica* **79(2)**: 164-167.
- 605 **Dong ZM, Sun YW, Wu SY. 2003.** On a new pterosaur from the Lower Cretaceous of Chaoyang
606 Basin, Western Liaoning, China. *Global Geology* **22(1)**: 1-8.
- 607 **Eberth DA, Russell DA, Braman DR, Deino AL. 1993.** The age of the dinosaur bearing
608 sediments at Tebch, Inner Mongolia, People's Republic of China. *Canadian Journal of Earth*
609 *Science* **30**: 2101–2106.
- 610 **Fastnacht M. 2001.** First record of *Coloborhynchus* (Pterosauria) from the Santana Formation
611 (Lower Cretaceous) of the Chapada do Araripe, Brazil. *Paläontologische Zeitschrift* **75(1)**:
612 23-26.
- 613 **Frey E, Martill DM, Buchy MC. 2003.** A new crested ornithocheirid from the Lower Cretaceous
614 of northeastern Brazil and the unusual death of an unusual pterosaur. *Geological Society,*
615 *London, Special Publications* **217(1)**: 55–63.

- 616 **Goloboff PA, Farris JS, Nixon KC. 2008.** TNT, a free program for phylogenetic
617 analysis. *Cladistics* **24(5)**: 774–786.
- 618 **Holgado B, Pêgas RV, Canudo JI, Fortuny J, Rodrigues T, Company J, Kellner AWA. 2019.**
619 On a new crested pterodactyloid from the Early Cretaceous of the Iberian Peninsula and the
620 radiation of the clade Anhangueria. *Scientific reports* **9(1)**: 4940.
- 621 **Howse SCB, Milner AR, Martill DM. 2001.** "Pterosaurs". In Martill D M, Naish D. *Dinosaurs*
622 *of the Isle of Wight*. The Palaeontological Association. Pp:324–335.
- 623 **Jiang SX, Wang XL, Meng X, Cheng X. 2014.** A new boreopterid pterosaur from the Lower
624 Cretaceous of western Liaoning, China, with a reassessment of the phylogenetic relationships
625 of the Boreopteridae. *Journal of Paleontology* **88(4)**: 823-828.
- 626 **Jiang SX, Cheng X, Ma YX, Wang XL. 2016.** A new archaeopterodactyloid pterosaur from the
627 Jiufotang Formation of western Liaoning, China, with a comparison of sterna in
628 Pterodactylomorpha. *Journal of Vertebrate Paleontology* **36 (6)**: e1212058.
- 629 **Kaup SS. 1834.** Versuch einer Eintheilung der Säugethiere in 6 Stämme und der Amphibien in 6
630 Ordnungen. *Isis von Oken, 1834, cols.* 311–315.
- 631 **Kellner AWA. 2003.** Pterosaur phylogeny and comments on the evolutionary history of the
632 group. Geological Society, London, Special Publications **217(1)**: 105–137.
- 633 **Kellner AWA. 2010.** Comments on the Pteranodontidae (Pterosauria, Pterodactyloidea) with the
634 description of two new species. *Anais da Academia Brasileira de Ciências* **82(4)**: 1063-1084.
- 635 **Kellner AWA. 2013.** A new unusual tapejarid (Pterosauria, Pterodactyloidea) from the Early
636 Cretaceous Romualdo Formation, Araripe Basin, Brazil. *Earth and Environmental Science*
637 *Transactions of the Royal Society of Edinburgh* **103(3-4)**: 409-421.
- 638 **Kellner AWA. 2017.** Rebuttal of Martin-Silverstone *et al.* 2017, 'Reassessment of *Dawndraco*
639 *kanzai* Kellner 2010 and reassignment of the type specimen to *Pteranodon sternbergi*
640 Harksen, 1966'. *Vertebrate Anatomy Morphology Palaeontology* **3**: 81-89.
- 641 **Kellner AWA, Tomida Y. 2000.** Description of a new species of Anhangueridae
642 (Pterodactyloidea) with comments on the pterosaur fauna from the Santana Formation
643 (Aptian–Albian), northeastern Brazil. *National Science Museum Monographs* **17**: ix-137.
- 644 **Li JJ, Lü JC, Zhang BK. 2003.** A new Lower Cretaceous sinopterid pterosaur from the western
645 Liaoning, China. *Acta Palaeontologica Sinica* **42(3)**: 442-447.
- 646 **Longrich NR, Martill DM, Andres B. 2018.** Late Maastrichtian pterosaurs from North Africa
647 and mass extinction of Pterosauria at the Cretaceous-Paleogene boundary. *PLoS Biology*
648 **16(3)**: e2001663.
- 649 **Lü JC. 2010.** A new boreopterid pterodactyloid pterosaur from the Early Cretaceous Yixian
650 Formation of Liaoning Province, northeastern China. *Acta Geologica Sinica* **84(2)**: 241-246.

- 651 **Lü JC, Fucha XH. 2010.** A new pterosaur (Pterosauria) from Middle Jurassic Tiaojishan
652 Formation of western Liaoning, China. *Global Geology* **13 (3/4)**: 113–118.
- 653 **Lü JC, Ji Q. 2005.** New azhdarchid pterosaur from the Early Cretaceous of western Liaoning.
654 *Acta Geologica Sinica* **79 (3)**: 301–307.
- 655 **Lü JC, Yuan CX. 2005.** New tapejarid pterosaur from western Liaoning, china. *Acta Geologica*
656 *Sinica* **79(4)**: 453-458.
- 657 **Lü JC, Jin XS, Unwin DM, Zhao LJ, Azuma Y, Ji Q. 2006.** A new species of *Huaxiapterus*
658 (Pterosauria: Pterodactyloidea) from the Lower Cretaceous of western Liaoning, China with
659 comments on the systematics of tapejarid pterosaurs. *Acta Geologica Sinica* **80(3)**: 315–326.
- 660 **Lü JC, Gao YB, Xing LD, Li ZX, Sun ZY. 2007.** A new species of *Huaxiapterus* from the Early
661 Cretaceous of western Liaoning, China. *Acta Geologica Sinica* **81 (5)**: 683–687.
- 662 **Lü JC, Xu L, Ji Q. 2008.** Restudy of *Liaoxipterus* (Istiodactylidae:Pterosauria), with comments
663 on the Chinese istiodactylid pterosaurs. *Zitteliana* **B28**: 229-241.
- 664 **Lü JC, Unwin DM, Jin XS, Liu YQ, Ji Q. 2009.** Evidence for modular evolution in a long-tailed
665 pterosaur with a pterodactyloid skull. *Proceedings of the Royal Society B: Biological*
666 *Sciences* **277(1680)**: 383-389.
- 667 **Lü JC, Xu L, Chang HL, Zhang XL. 2011.** A new darwinopterid pterosaur from the Middle
668 Jurassic of western Liaoning, northeastern China and its ecological implications. *Acta*
669 *Geologica Sinica* **85(3)**: 507-514.
- 670 **Lü JC, Jin XS, Gao CL, Du TM, Ding M, Sheng YM, Wei XF. 2013.** *Dragons of the Skies*
671 *(Recent advances on the study of pterosaurs from China)*. Zhejiang Science & Technology
672 Press. 127 Pp.
- 673 **Lü J C, Liu C Y, Xu L, Pan L J, Shen C Z. 2016a.** A new pterodactyloid pterosaur from the
674 Early Cretaceous of the Western Part of Liaoning Province, Northeastern China. *Acta*
675 *Geologica Sinica*, **90 (3)**: 777–782.
- 676 **Lü J C, Teng F F, Sun D Y, Shen C Z, Li G Q, Gao X, Liu H F. 2016b.** The toothless pterosaurs
677 from China. *Acta Geologica Sinica*, **90 (9)**: 2513–2525.
- 678 **Martill DM. 2011.** A new pterodactyloid pterosaur from the Santana Formation (Cretaceous) of
679 Brazil. *Cretaceous Research* **32 (2)**: 236-243.
- 680 **Martill DM. 2014.** A functional odontoid in the dentary of the Early Cretaceous pterosaur
681 *Istiodactylus latidens*: Implications for feeding. *Cretaceous Research* **47**: 56-65.
- 682 **Martill DM, Etches S. 2013.** A new monofenestratan pterosaur from the Kimmeridge Clay
683 Formation (Kimmeridgian, Upper Jurassic) of Dorset, England. *Acta Palaeontologica*
684 *Polonica* **58(2)**: 285-295.

- 685 **Martin-Silverstone E, Glasier JRN, John H. Acorn JH, Mohr S, Currie PJ. 2017.**
686 Redescription of *Dawndraco kanzai* Kellner, 2010 and reassignment of the type specimen to
687 *Pteranodon sternbergi* Harksen, 1966. *Vertebrate Anatomy Morphology Palaeontology* **3**:
688 47-59.
- 689 **Meng J, Wang YQ, Li CK. 2011.** Transitional mammalian middle ear from a new Cretaceous
690 Jehol eutriconodont. *Nature* **472(7342)**: 181–185.
- 691 **Pêgas RV, Costa FR, Kellner AWA. 2018.** New information on the osteology and a taxonomic
692 revision of the genus *Thalassodromeus* (Pterodactyloidea, Tapejaridae,
693 Thalassodrominae). *Journal of Vertebrate Paleontology* **38(2)**: e1443273.
- 694 **Pinheiro FL, Rodrigues T. 2017.** *Anhanguera* taxonomy revisited: is our understanding of
695 Santana Group pterosaur diversity biased by poor biological and stratigraphic
696 control? *PeerJ* **5**: e3285.
- 697 **Pinheiro FL, Schultz CL. 2012.** An unusual pterosaur specimen (Pterodactyloidea,
698 Azhdarchoidea) from the Early Cretaceous Romualdo Formation of Brazil, and the evolution
699 of the pterodactyloid palate. *PLOS ONE* **7(11)**: e50088.
- 700 **Plieninger F. 1901.** Beiträge zur Kenntnis der Flugsaurier. *Palaeontographica* **48**: 65–90.
- 701 **Rodrigues T, Kellner AWA. 2013.** Taxonomic review of the *Ornithocheirus* complex
702 (Pterosauria) from the Cretaceous of England. *ZooKeys* **308**: 1–112.
- 703 **Rodrigues T, Jiang SX, Cheng X, Wang X, Kellner AWA. 2015.** A new toothed pteranodontoid
704 (Pterosauria: Pterodactyloidea) from the Jiufotang Formation (Lower Cretaceous, Aptian) of
705 China and comments on *Liaoningopterus gui* Wang and Zhou, 2003. *Historical Biology*
706 **27(6)**: 782-795.
- 707 **Seeley HG. 1901.** *Dragons of the Air. An account of extinct flying reptiles.* Methuen, London, xiii
708 p 239 pp.
- 709 **Sullivan C, Wang Y, Hone DW, Wang YQ, Xu X, Zhang FC. 2014.** The vertebrates of the
710 Jurassic Daohugou Biota of northeastern China. *Journal of Vertebrate Paleontology* **34(2)**:
711 243-280.
- 712 **Unwin DM. 2003.** On the phylogeny and evolutionary history of pterosaurs. Geological Society,
713 London, Special Publications **217(1)**: 139-190.
- 714 **Vidovic SU, Martill DM. 2014.** *Pterodactylus scolopaciceps* Meyer, 1860 (Pterosauria,
715 Pterodactyloidea) from the Upper Jurassic of Bavaria, Germany: the problem of cryptic
716 pterosaur taxa in early ontogeny. *PloS one* **9(10)**: e110646.
- 717 **Wang L, Li L, Duan Y, Cheng SL. 2006.** A new istiodactylid pterosaur from western Liaoning,
718 China. *Geological Bulletin of China* **25(6)**: 737-740.
- 719 **Wang M, Zhou ZH. 2019.** A new enantiornithine (Aves: Ornithothoraces) with completely fused

- 720 premaxillae from the Early Cretaceous of China. *Journal of Systematic Palaeontology Online*
721 **edition:** 1–14.
- 722 **Wang X. 2018.** Background for the Plant Fossils. Pp. 47-59 in: *The Dawn Angiosperms*. Springer
723 Geology. Springer, Cham. 334 Pp.
- 724 **Wang XL, Lü JC. 2001.** Discovery of a pterodactylid pterosaur from the Yixian Formation of
725 western Liaoning, China. *Chinese Science Bulletin* **46(13)**: 1112-1117.
- 726 **Wang XL, Zhou ZH. 2003a.** A new pterosaur (Pterodactyloidea, Tapejaridae) from the Early
727 Cretaceous Jiufotang Formation of Western Liaoning, China and its implications for
728 biostratigraphy. *Chinese Science Bulletin* **48(1)**: 16-23.
- 729 **Wang XL, Zhou ZH. 2003b.** Two new pterodactyloid pterosaurs from the Early Cretaceous
730 Jiufotang Formation of Western Liaoning, China. *Vertebrata Palasiatica* **41 (1)**: 34–41.
- 731 **Wang XL, Kellner AWA, Zhou ZH, Campos DA. 2005.** Pterosaur diversity and faunal turnover
732 in Cretaceous terrestrial ecosystems in China. *Nature* **437**: 875-879.
- 733 **Wang XL, Campos DA, Zhou ZH, Kellner AWA. 2008a.** A primitive istiodactylid pterosaur
734 (Pterodactyloidea) from the Jiufotang Formation (Early Cretaceous), northeast China.
735 *Zootaxa* **1813**: 1-18.
- 736 **Wang XL, Kellner AWA, Zhou ZH, Campos DA. 2008b.** Discovery of a rare arboreal forest-
737 dwelling flying reptile (Pterosauria: Pterodactyloidea) from China. *Proceedings of the*
738 *National Academy of Sciences* **105(6)**: 1983-1987
- 739 **Wang XL, Kellner AWA, Jiang SX, Meng X. 2009.** An unusual long-tailed pterosaur with
740 elongated neck from western Liaoning of China. *Anais da Academia Brasileira de*
741 *Ciências* **81(4)**: 793-812.
- 742 **Wang XL, Kellner AWA, Jiang SX, Cheng X, Meng X, Rodrigues T. 2010.** New long-tailed
743 pterosaurs (Wukongopteridae) from western Liaoning, China. *Anais da Academia Brasileira*
744 *de Ciências* **82(4)**: 1045-1062.
- 745 **Wang XL, Kellner AWA, Jiang SX, Cheng X. 2012.** New toothed flying reptile from Asia; close
746 similarities between early Cretaceous pterosaurs faunas from China and Brazil.
747 *Naturwissenschaften* **99(4)**: 249-257.
- 748 **Wang XL, Kellner AWA, Jiang SX, Wang Q, Ma YX, Paidoula Y, Cheng X, Rodrigues T,**
749 **Meng X, Zhang JL, Li N, Zhou ZH. 2014.** Sexually dimorphic tridimensionally preserved
750 pterosaurs and their eggs from China. *Current Biology* **24(12)**: 1323-1330.
- 751 **Wang XL, Rodrigues T, Jiang SX, Cheng X, Kellner AWA. 2015.** An Early Cretaceous
752 pterosaur with an unusual mandibular crest from China and a potential novel feeding strategy.
753 *Scientific Reports* **4**: 6329.
- 754 **Wellnhofer P. 1987.** New crested pterosaurs from the Lower Cretaceous of Brazil. *Mitteilungen*

- 755 der Bayerischen Staatssammlung für Paläontologie und Historische Geologie **27**:17–186.
- 756 **Witton MP. 2012.** New insights into the skull of *Istiodactylus latidens* (Ornithocheiroidea,
757 Pterodactyloidea). PloS one **7(3)**: e33170.
- 758 **Wu ZJ, Gao FL, Pan YQ, Wang X. 2018.** Division and comparison of Jiufotang Formation of
759 western Liaoning area and its rare fossil bed. Geoscience **32(4)**: 758–765.
- 760 **Xu X, Zhou Z, Wang X, Kuang X, Zhang F, Du X. 2003.** Four-winged dinosaurs from
761 China. Nature **421(6921)**: 335.
- 762 **Yao X, Liao CC, Sullivan C, Xu X. 2019.** A new transitional therizinosaurian theropod from the
763 Early Cretaceous Jehol Biota of China. Scientific Reports **9**: 5026
- 764 **Zhou ZH, Barrett PM, Hilton J. 2003.** An exceptionally preserved Lower Cretaceous ecosystem.
765 Nature **421(6925)**: 807–814.

766

767 **Figures**

768 **Figure 1. *Nurhachius luei* sp. nov., BPMC-0204, holotype, photograph and line drawing.** The
769 scale bar in the line drawing equals 50 mm. Abbreviations: alv, alveolus; an, angular; art, articular;
770 ax, axis; ceI, ceratobranchial I; ch, choana; cv, cervical vertebra; d, dentary; f, frontal; j, jugal; la,
771 lacrimal; m, maxilla; n, nasal; naof, nasoantorbital fenestra; odp, odontoid process; or, orbit; pa,
772 parietal; pf, prefrontal; pmax, premaxilla; po, postorbital; prid, palatal ridge; pty, pterygoid; q,
773 quadrate; vo, vomer. Isolated numbers indicate tooth positions. Note: the visible region of the
774 pterygoid corresponds to the medial process of the bone. Photo by Xuanyu Zhou. Drawing by
775 Maria Eduarda Leal.

776

777 **Figure 2. Location of the site where BPMC-0204 was found.**

778

779 **Figure 3. *Nurhachius ignaciobrito* specimens, photographs and line drawings.** (A) LPM
780 00023, referred specimen (holotype of *Longchengpterus zhaoui*), skull and mandible in right lateral
781 view. (B) IVPP V-13288, holotype, skull (mirrored) and mandible in right lateral view. Scale bars
782 equal 50 mm. Abbreviations: art, articular; ch, choana; d, dentary; f, frontal; ios, interorbital
783 septum; j, jugal; ls, laterosphenoid; m, maxilla; n, nasal; op, opisthotic; or, orbit; pa, parietal; pf,
784 prefrontal; pm, premaxilla; prid, palatal ridge; pty, pterygoid; q, quadrate; san, surangular; sq,
785 squamosal. Photographs by Xuanyu Zhou. Drawings by Rodrigo V. Pêgas.

786

787 **Figure 4. Close view of the rostral tip of *Nurhachius* species in right lateral view.** (A)
788 *Nurhachius luei* sp. nov., holotype and (C) *Nurhachius ignaciobritoi*, IVPP V-13288, holotype,
789 mirrored. (B) and (D), respective schematic drawings of (A) and (C), showing the slight dorsal
790 deflection of the palatal anterior tip (notice the positions of the first and second alveoli in both
791 specimens). Numbers indicate tooth positions. Scale bars equal 20 mm. Photos by Xuanyu Zhou.
792 Drawings by Rodrigo V. Pêgas.

793

794 **Figure 5. Close view of the dentary symphysis of *Nurhachius* species.** (A) *Nurhachius luei* sp.
795 nov. holotype in dorsolateral view, and (B) line drawing. (C) *Nurhachius ignaciobritoi*, LPM
796 00023, referred specimen, occlusal view, and (D), line drawing. Abbreviations: mg, median
797 groove; odp, odontoid process. Numbers indicate tooth positions. Red arrows indicate the
798 mesiodistal constriction between crown and root. Photos by Xuanyu Zhou. Drawings by Maria
799 Eduarda Leal and Rodrigo V. Pêgas.

800

801 **Figure 6. Close view of the dentition in *Nurhachius* species.** (A) *Nurhachius ignaciobritoi*, LPM
802 00023, referred specimen, isolated tooth in lingual view, and (B) line drawing. (C) *Nurhachius*
803 *luei* sp. nov. holotype, ninth left mandibular tooth in lingual view, and (D) line drawing. Red
804 arrows indicate the mesiodistal constrictions between crown and root. Blue arrows indicate the
805 horizontal elevation at the base of the crown (cingulum). Photos by Xuanyu Zhou. Drawings by
806 Rodrigo V. Pêgas.

807

808 **Figure 7. *Nurhachius luei* sp. nov. phylogenetic relationships.** Strict consensus tree of 51 most
809 parsimonious trees. Tree length is 358, consistency index 0.644 and retention index 0.867. The red
810 rectangle indicates the Istiodactylidae and its two closest taxa.

811

812 **Figure 8. Other istiodactylids and close taxa.** (A) *Liaoxipterus brachyognathus*, CAR-0018,
813 holotype, lower jaw in dorsal view. (B) *Haopterus gracilis*, IVPP V11726, holotype, skull in right
814 lateral view. (C) *Hongshanopterus lacustris*, IVPP V14582, holotype, skull in ventral view. All
815 scale bars equal 50 mm. (A) and (C) by Xuanyu Zhou; (B) by Shunxing Jiang (courtesy of IVPP).

816

Figure 1

Nurhachius luei sp. nov., BPMC-0204, holotype, photograph and line drawing.

The scale bar in the line drawing equals 50 mm. Abbreviations: alv, alveolus; an, angular; art, articular; ax, axis; cel, ceratobranchial I; ch, choana; cv, cervical vertebra; d, dentary; f, frontal; j, jugal; la, lacrimal; m, maxilla; n, nasal; naof, nasoantorbital fenestra; odp, odontoid process; or, orbit; pa, parietal; pf, prefrontal; pmax, premaxilla; po, postorbital; prid, palatal ridge; pty, pterygoid; q, quadrate; vo, vomer. Isolated numbers indicate tooth positions.

Note: the visible region of the pterygoid corresponds to the medial process of the bone.

Photo by Xuanyu Zhou. Drawing by Maria Eduarda Leal.

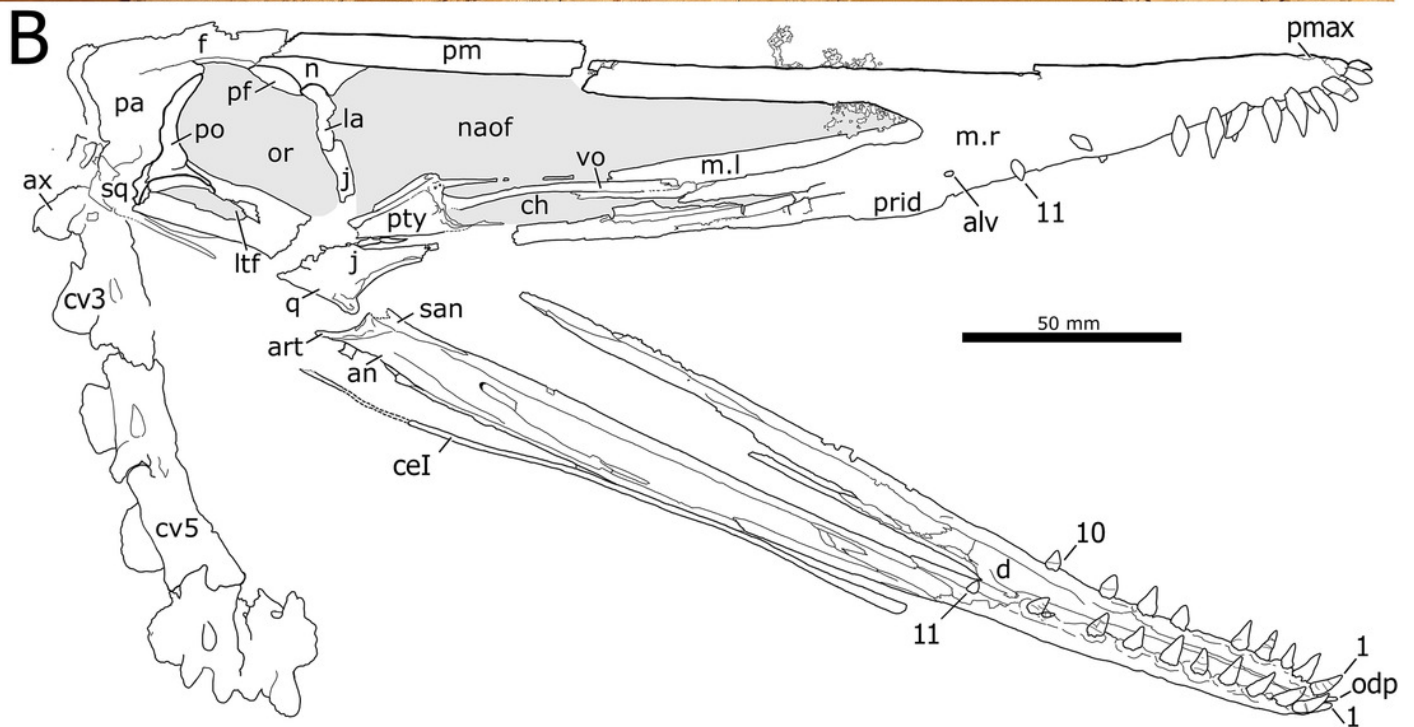


Figure 2

Location of the site where BPMC-0204 was found.

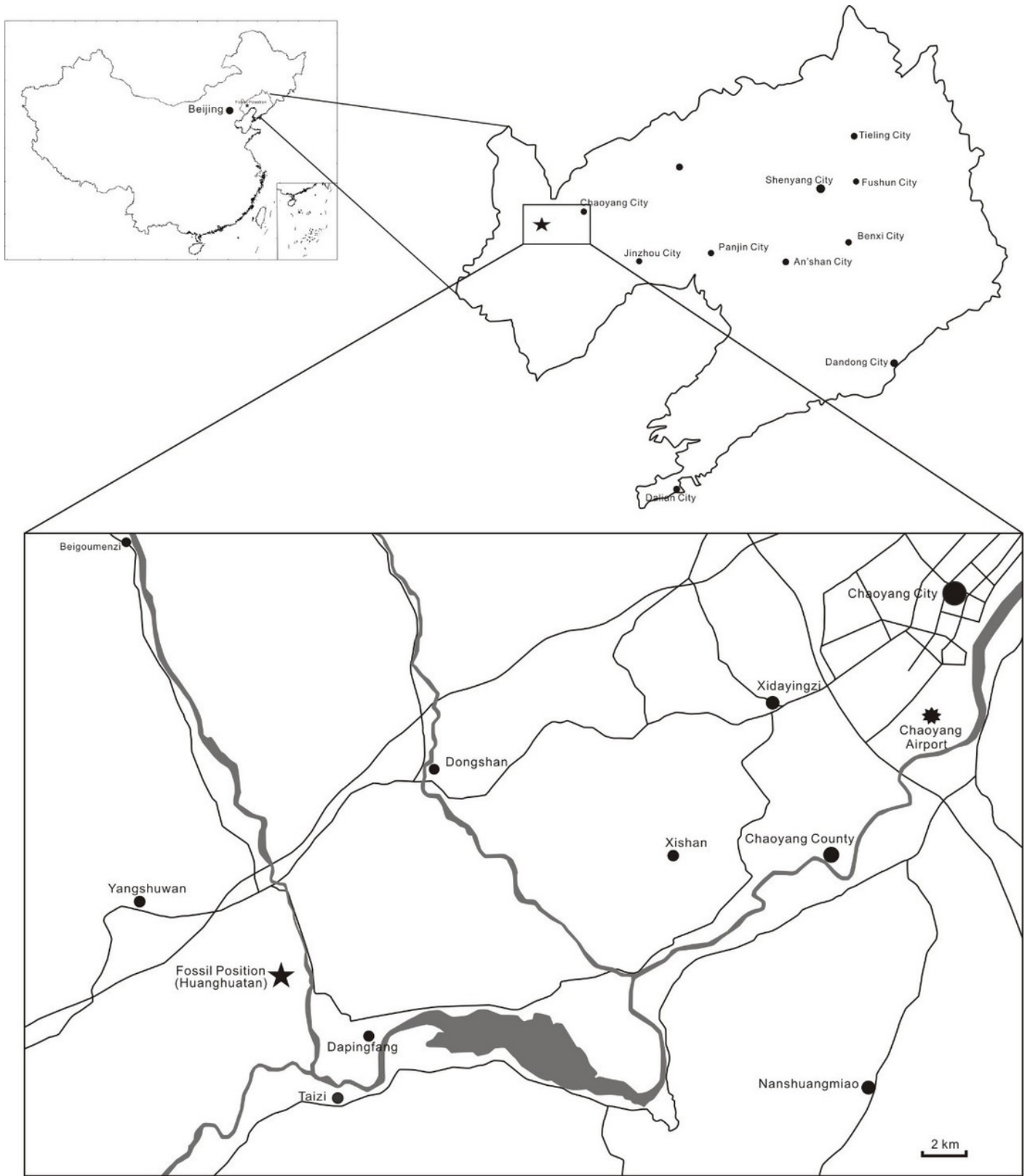


Figure 3

Nurhachius ignaciobrito specimens, photographs and line drawings.

(A) LPM 00023, referred specimen (former holotype of "*Longchengpterus zhaoi*"), skull and mandible in right lateral view; and (B) interpretative line drawing. (C) IVPP V-13288, holotype, skull (mirrored) and mandible in right lateral view; and (D) interpretative line drawing. Scale bars equal 50 mm. Abbreviations: art, articular; ch, choana; d, dentary; f, frontal; ios, interorbital septum; j, jugal; ls, laterosphenoid; m, maxilla; n, nasal; op, opisthotic; or, orbit; pa, parietal; pf, prefrontal; pm, premaxilla; prid, palatal ridge; pty, pterygoid; q, quadrate; san, surangular; sq, squamosal. Photographs by Xuanyu Zhou. Drawings by Rodrigo V. Pêgas.

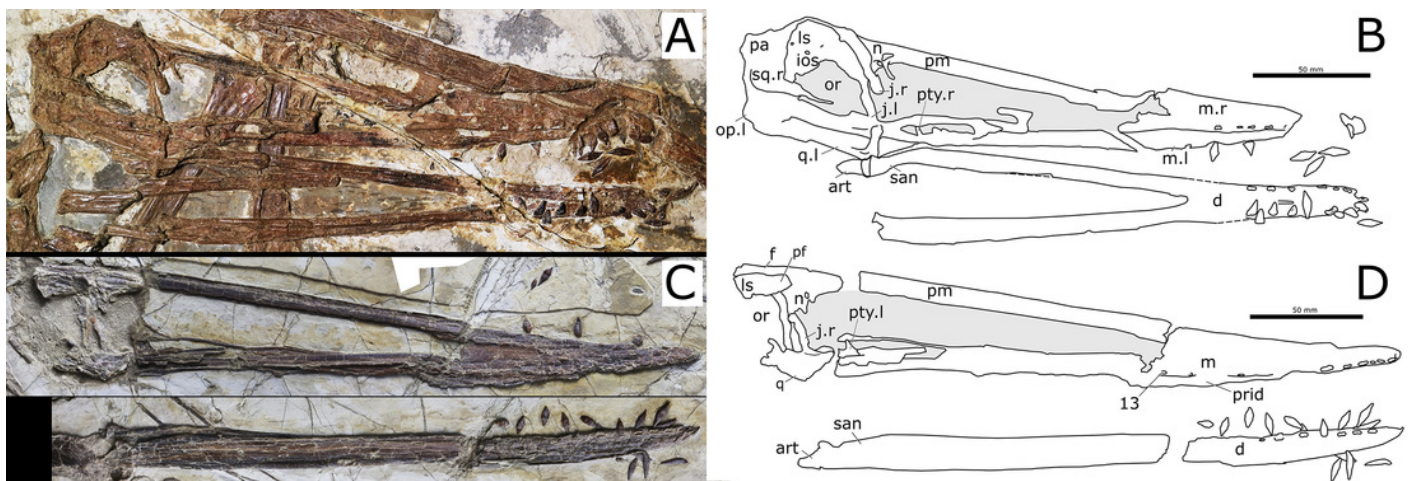


Figure 4

Close view of the rostral tip of *Nurhachius* species in right lateral view.

(A) *Nurhachius luei* sp. nov., holotype and (C) *Nurhachius ignaciobritoj*, IVPP V-13288, holotype, mirrored. (B) and (D), respective schematic drawings of (A) and (C), showing the slight dorsal deflection of the palate (notice the positions of the first and second alveoli in both specimens). Numbers indicate tooth positions. Scale bars equal 20 mm. Photos by Xuanyu Zhou. Drawings by Rodrigo V. Pêgas.

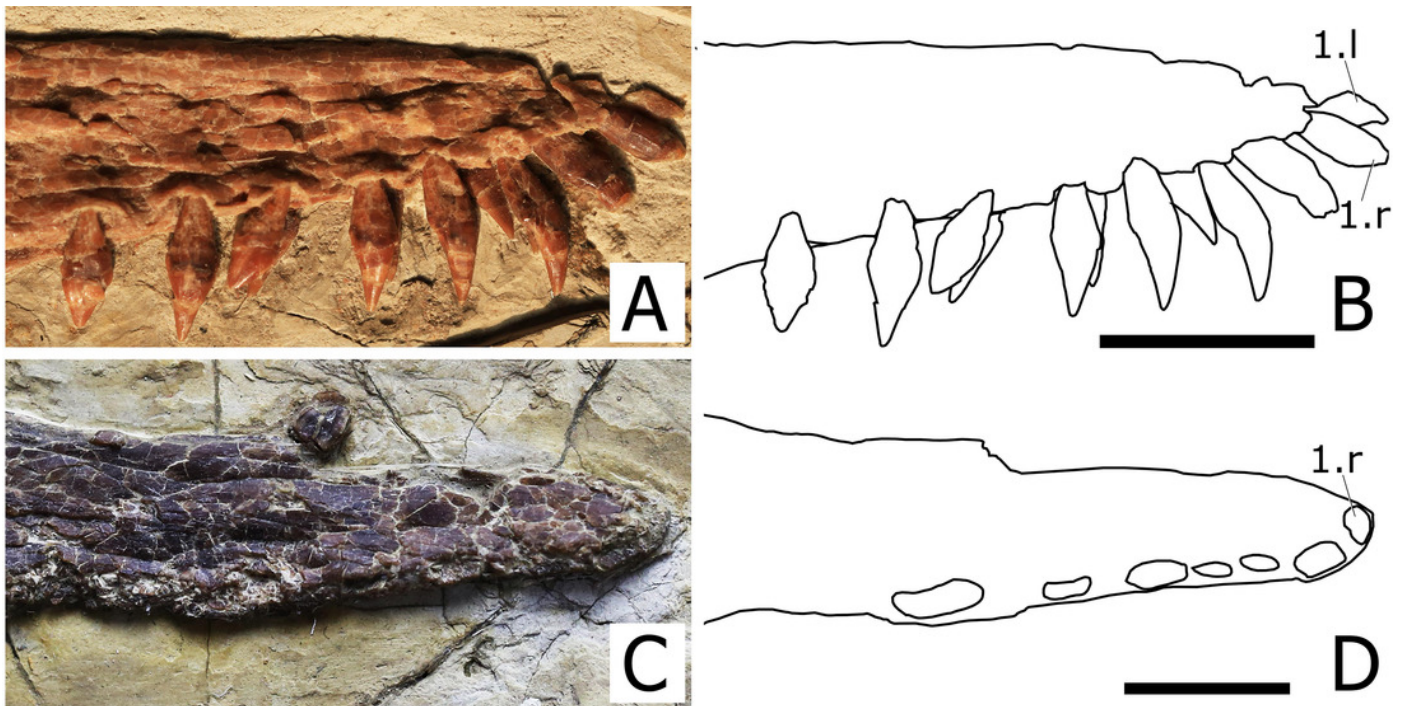


Figure 5

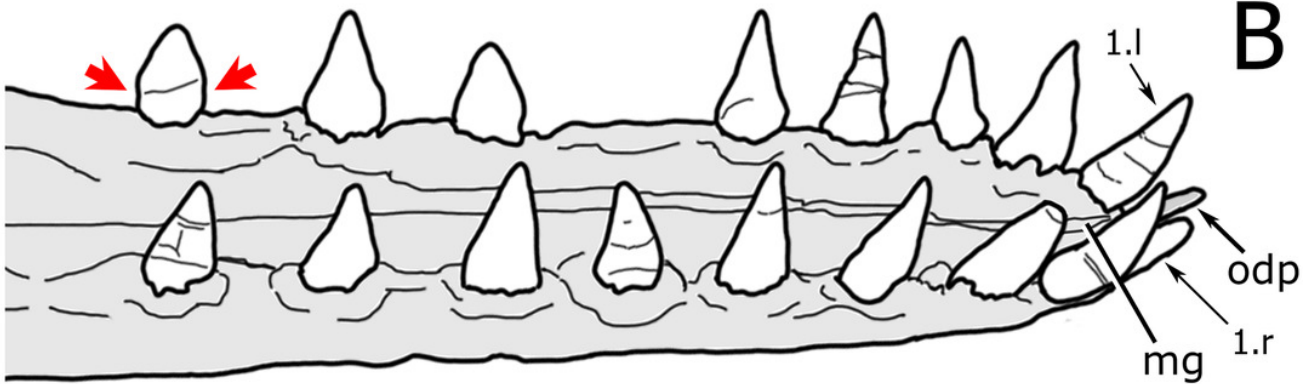
Close view of the dentary symphysis of *Nurhachius* species.

(A) *Nurhachius luei* sp. nov. holotype in dorsolateral view, and (B) line drawing. (C) *Nurhachius ignaciobrito*, LPM 00023, referred specimen, occlusal view, and (D), line drawing.

Abbreviations: mg, median groove; odp, odontoid process. Numbers indicate tooth positions. Red arrows indicate the mesiodistal constriction between crown and root. Photos by Xuanyu Zhou. Drawings by Maria Eduarda Leal and Rodrigo V. Pêgas.



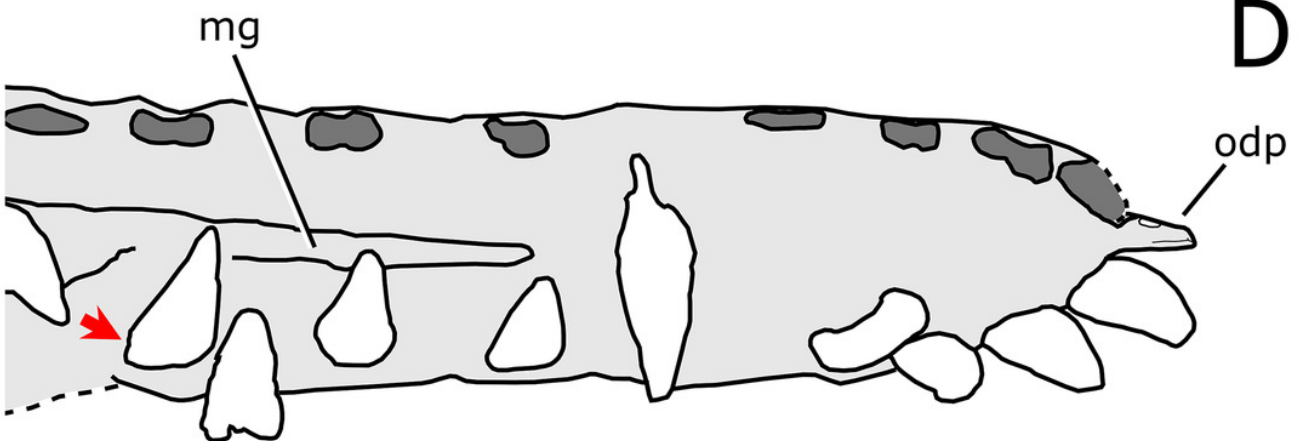
A



B



C



D

Figure 6

Nurhachius luei sp. nov. phylogenetic relationships.

Strict consensus tree of 51 most parsimonious trees. Tree length is 360, consistency index 0.642 and retention index 0.864. The red rectangle indicates the Istiodactylidae and its two closest taxa.

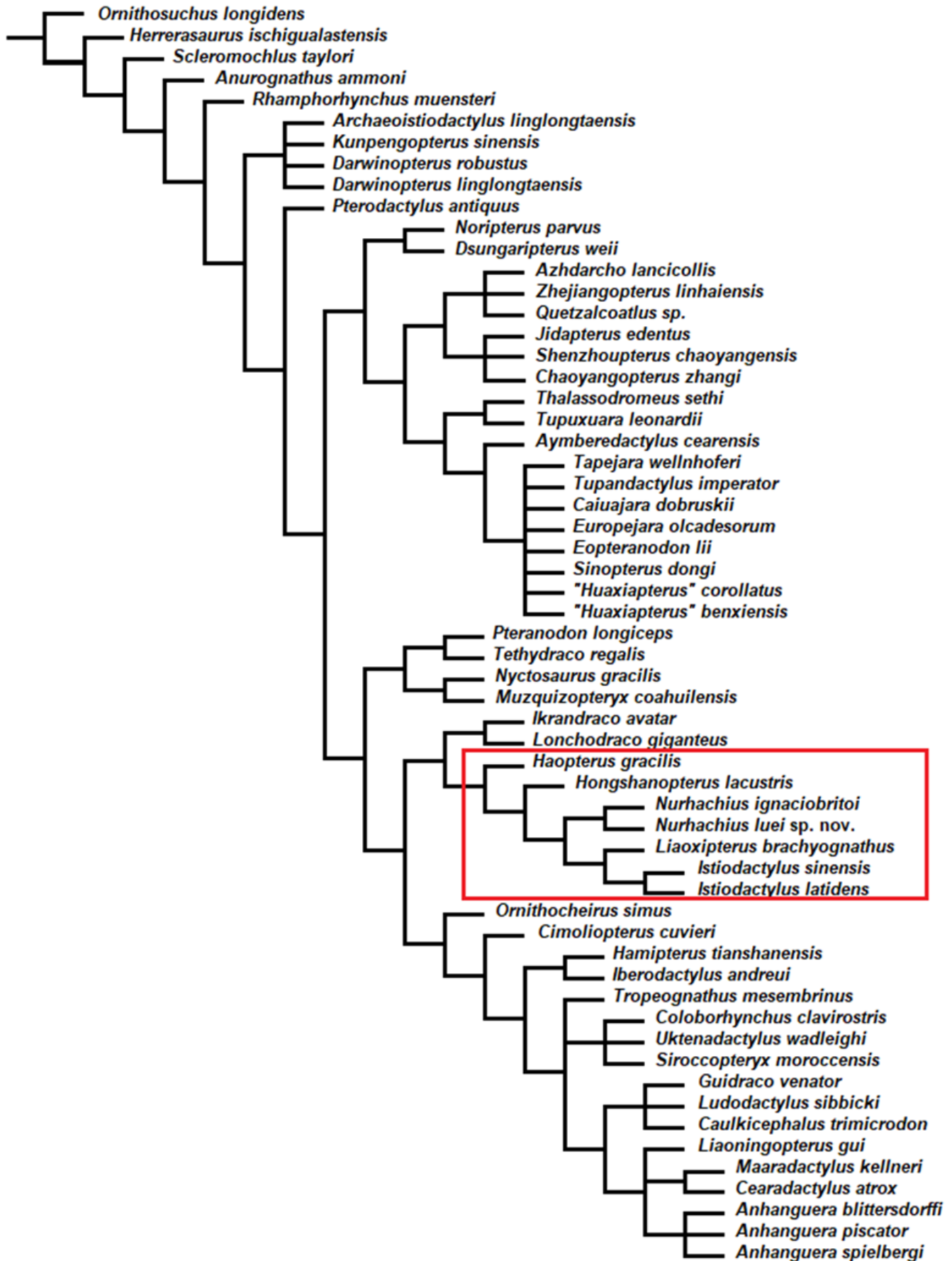


Figure 7

Close view of the dentition in *Nurhachius* species.

(A) *Nurhachius ignaciobritoi*, LPM 00023, referred specimen, isolated tooth in lingual view, and (B) line drawing. (C) *Nurhachius luei* sp. nov. holotype, ninth left mandibular tooth in lingual view, and (D) line drawing. Red arrows indicate the mesiodistal constrictions between crown and root. Blue arrows indicate the horizontal elevation at the base of the crown (cingulum). Photos by Xuanyu Zhou. Drawings by Rodrigo V. Pêgas.

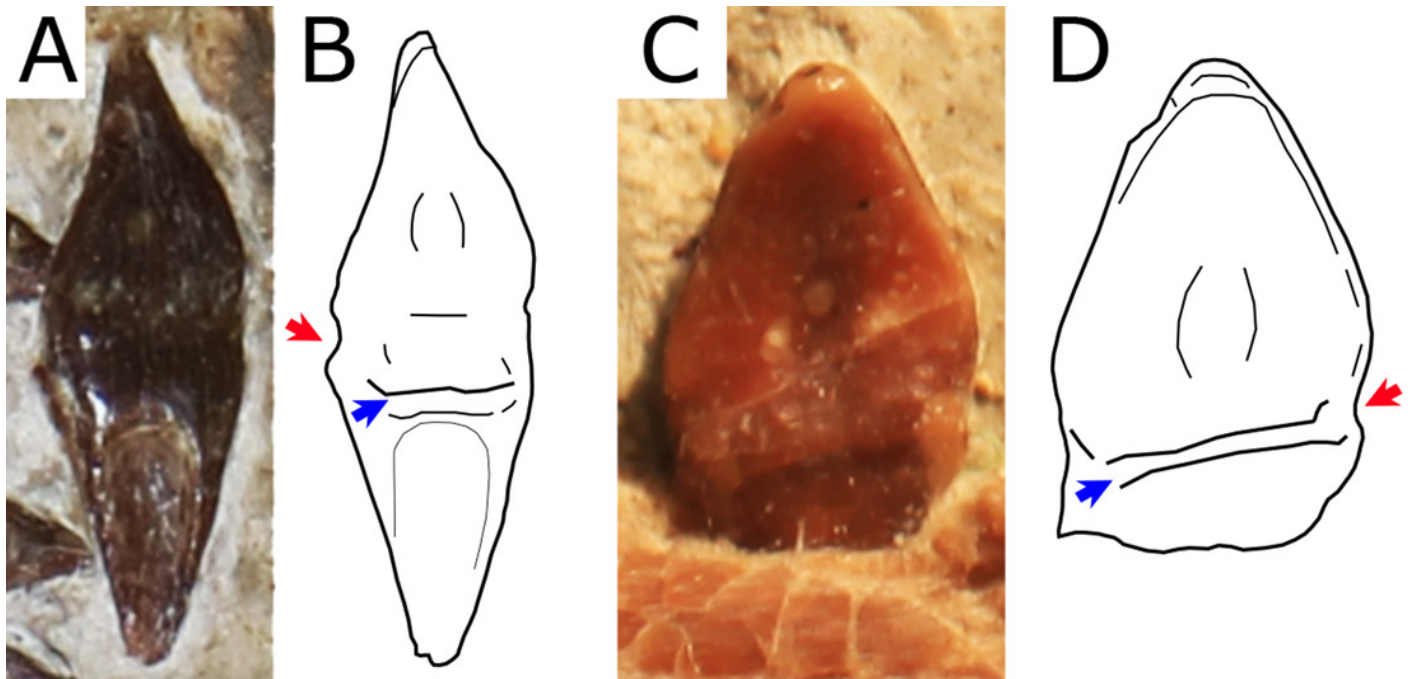


Figure 8

Other istiodactylids and close taxa.

(A) *Liaoxipterus brachyognathus*, CAR-0018, holotype, lower jaw in dorsal view. (B) *Haopterus gracilis*, IVPP V11726, holotype, skull in right lateral view. (C) *Hongshanopterus lacustris*, IVPP V14582, holotype, skull in ventral view. All scale bars equal 50 mm. (A) and (C) by Xuanyu Zhou; (B) by Shunxing Jiang (courtesy of IVPP).

